Research Article

Xiaolong Sun, Yunchu Zhu, Jie Mao, Xiao Qin*, Lijuan Li, Jiao Jin, and Huayang Yu

# UV aging behavior evolution characterization of HALS-modified asphalt based on micro-morphological features

https://doi.org/10.1515/rams-2023-0109
received March 28, 2023; accepted July 26, 2023

**Abstract:** To clarify the effect of Hindered amine light stabilizer (HALS) on ultraviolet (UV) aging behavior of asphalt binder, the evolution history and characteristics of the UV induced micro-structure of modified asphalt were characterized. Scanning Electron Microscope (SEM) and Atomic Force Microscope (AFM) were used to analyze the microscopic morphology evolution of light stabilizer-modified asphalt during UV aging. By defining the micro-structure of asphalt in aging joints induced by UV, the identification and classification of typical micro-structure are proposed. On this basis, an evaluation method based on the morphology evolution process of modified asphalt aging was proposed to quantitatively analyze the effect of HALS on the UV aging of asphalt binder. The results show that the control effect of HALS on the UV aging behavior of asphalt can be verified by SEM and AFM detection methods. At the same time, the aging interval of the asphalt modified by hindered amine was divided by the method, and it was verified that the HALS could significantly prolong the service life of the asphalt binder. The micro-morphology of asphalt binder undergoes the process of crack generation and propagation during UV aging. The micro-morphological changes of UV aged asphalt were interfered effectively by HALS, which could alleviate and control the development of UV induced micro-cracks, and promote the fusion of micro-cracks. This study provides an effective evaluation method for detecting UV aging microscopic evolution of HALS.

**Keywords:** UV aging, quantitative characterization, hindered amine light stabilizer

## 1 Introduction

Asphalt, as a high-viscosity organic material composed of hydrocarbons and their non-metallic derivatives, has been widely used as a pavement material in the field of road engineering [1]. However, when exposed to the elements such as light, heat, and water, the performance of asphalt pavement materials decreases. Especially under intense ultraviolet (UV) radiation, the chemical structure of asphalt pavement is damaged, which induces chemical reactions such as molecular alienation and dehydrogenation, accelerates the aging and cracking of asphalt pavement, seriously degrades the comprehensive performance of asphalt pavement, and makes the durability of asphalt pavement difficult to meet the design requirements [2, 3]. Therefore, controlling the road defects caused by UV aging of asphalt is the key to prolonging the service life of asphalt pavement.

At present, improving the anti-UV aging ability of asphalt is the main way to control the UV aging behavior of asphalt, which is achieved by adding various anti-aging agents [4]. The existing anti-UV additives include UV absorbent, antioxidant, composite-modified asphalt, or light stabilizers, among which Hindered amine light stabilizer (HALS) shows excellent anti-UV aging ability, can realize the extension of service life, and improve the use efficiency of asphalt roads [5–7].

Scholars at home and abroad have studied the anti-UV aging effect of HALS-modified asphalt. The results show

* **Corresponding author: Xiao Qin**, School of Transportation and Civil Engineering and Architecture, Foshan University, Foshan 528000, China, e-mail: qinnao@126.com
**Xiaolong Sun:** School of Civil and Transportation Engineering, Guangdong University of Technology, Guangzhou, 510006, China; National Engineering Research Center of Highway Maintenance Technology, Changsha University of Science & Technology, Changsha, 410114, Hunan, China
**Yunchu Zhu, Lijuan Li:** School of Civil and Transportation Engineering, Guangdong University of Technology, Guangzhou, 510006, China
**Jie Mao:** Guangdong Guan Yue Highway & Bridge Co., Ltd, Guangzhou, 511450, China
**Jiao Jin:** National Engineering Research Center of Highway Maintenance Technology, Changsha University of Science & Technology, Changsha, 410114, Hunan, China
**Huayang Yu:** School of Civil Engineering and Transportation, South China University of Technology, Guangzhou, 510641, China

that the HALS can provide anti-aging ability for some time, but this ability gradually fails with aging time. Therefore, extending the anti-aging stage of photostable modified asphalt is the key to improving the UV aging degree of asphalt. It is the premise of improving the efficiency of asphalt roads to detect the failure time of anti-UV aging ability of modified asphalt.

Recently, many macro and micro detection technologies have been used to monitor the aging process of asphalt materials [8–13]. Therefore, it is the key to study the evolution process of the micro-morphology of modified asphalt under UV aging to select appropriate micro-detection means and to propose regular evaluation parameters.

Different technical detection means have different research indexes. Chen studied the aging degree of different asphalt layers by Fluorescence Microscopy (FM) to characterize the aging difference [14]. Because the asphalt has a "gradient effect" in the face of UV light, FM can detect that the phosphor in the asphalt gradually deepens from the surface to the inside, which indicates that the aging process of the asphalt is the same. Zeng also reported that the same research results can also be obtained by using an UV spectrophotometer and stripping technology, since the direct influence of UV radiation on asphalt is only reflected in the surface layer [15]. Atomic Force Microscope-Infrared Spectroscopy (AFM-IR) was used by Xing to analyze and evaluate the results of asphalt materials before and after UV aging [16]. According to the results of infrared spectrogram characterization, it can be found that carbonyl and sulfoxide groups increase significantly in each component of asphalt after UV radiation, that is, an oxidation reaction occurs in each component. For the Cryo-scanning electron microscopy (Cryo-SEM), Mokhtari evaluated the aging and regeneration properties of asphalt surface cracks by observing the fracture surface, crevice, and texture analysis results of the images [17].

Among them, SEM and AFM detection methods, due to their convenience and intuitiveness, are usually used to analyze the characterization results of asphalt surface micro-morphology, surface roughness, adhesion, and other indicators at a microscopic scale [14]. AFM was used to identify the effect of UV aging on the chemical properties of asphalt, and it is believed that the formation of a "bee-like" structure is related to asphaltene. The lightweight components in asphalt gradually decrease with age, and the proportion of recombination components increases. After aging, the surface roughness and adhesive force of asphalt are reduced [21, 22]. The micro-structure of AFM is closely related to the composition of asphalt [23]. By studying the microscopic morphology of asphalt materials at different aging stages, it is inferred that the formation of bee structure comes from the formation of asphaltene and part of gum. The change in asphalt micro-structure is the direct manifestation of asphalt aging. The SEM characterization method can be used to evaluate the properties of asphalt that are affected by UV aging on the microscopic scale. Asphalt materials' most prominent morphological changes under UV aging can be reflected by the expansion degree of cracks. Observing the morphological changes of asphalt materials at the microscopic level, SEM detection can directly discover the cracks on the microscopic surface.

Therefore, based on the research status of micro detection technology at home and abroad, this study uses SEM and AFM detection technology to measure the micro-topography, to define the aging evolution process of modified asphalt. A comprehensive and accurate method was proposed to study the UV aging behavior of asphalt modified by HALS based on the microscopic characteristics. On this basis, combined with the change law of surface roughness of asphalt modified by light stabilizer in UV aging process, the influence law of HALS on the micro-structure evolution behavior of asphalt binder under UV condition was analyzed, and the applicability and feasibility of the physical preparation method proposed in this study were confirmed.

# 2 Test materials and research methods

## 2.1 Raw materials and preparation

### 2.1.1 Raw materials

#### 2.1.1.1 70# base asphalt

The 70# base asphalt was used as the carrier asphalt to prepare the modified asphalt. The three indexes of the unaged matrix asphalt and the matrix asphalt after 305 h UV aging were tested.

#### 2.1.1.2 HALS

HALS has certain chemical stability and high-temperature resistance. Tinuvin770 (T770) and Tinuvin622 (T622) HALS are selected as modifiers. The technical performance indexes are shown in Table 1. According to the previous research results, the application content of T770 and T622 light stabilizers is about 0.4% of the asphalt mass [12].

**Table 1:** Properties index of HALS

| Name | Appearance | Melting point (°C) | Molecular formula | Molecular weight |
|---|---|---|---|---|
| T770 | White powder | 82–85 | $C_{28}H_{52}O_4N_2$ | 480.7 |
| T622 | White crystalline powder | >350 | $C_{15}H_{29}NO_6$ | 319.4 |

#### 2.1.2 Preparation of asphalt UV aging specimens modified by HALS

##### 2.1.2.1 Preparation of modified asphalt

The specific preparation process of light stabilizer-modified asphalt: First, 70 # base asphalt was placed in an incubator at 135°C for 1.5 h. The asphalt was then poured into a clean beaker. The beaker was kept warm in an oil bath heater at 160 ± 5°C. The HALS with a mass fraction of 0.4% asphalt was prepared. Then, the light stabilizer (T770 or T622) was added to the molten asphalt. The beakers were placed in oil thermostat and heated and mixed for 10 min at a shear rate of 5,000 rad·min$^{-1}$. Third, the prepared modified asphalt with HALS was put into an oven at 115°C and swelled for 1.5 h to complete the preparation of modified asphalt material.

To complete the preparation of UV aging film samples, different UV aging time was set for asphalt film samples. Preparation process of UV aged film sample: First, the liquid-modified asphalt was dropped on the glass slide using an eyedropper. Wait for the asphalt to self-level at room temperature. Then, the asphalt sample was put into the UV aging test chamber for UV radiation treatment. Figure 1 shows the specific preparation process of the complete light stabilizer-modified asphalt sample.

##### 2.1.2.2 UV aging disposal and sample preparation

The annual average unit radiation intensity in areas with intense UV radiation intensity was mostly 7,000 MJ·m$^{-2}$. In order to simulate the influence of UV radiation on modified asphalt pavement materials indoor, the average unit UV radiation intensity was about 420 MJ·m$^{-2}$. The UV Weatherability Test Chamber was selected as the test equipment in this study. The output power of the test equipment is about 300 W, the radiation area is 0.8 m$^2$, and its UV radiation intensity is about 375 W·m$^{-2}$. Table 2 shows the relationship between indoor aging time and application environment aging time.

## 2.2 Test methods

### 2.2.1 Test equipment

#### 2.2.1.1 SEM analysis

SEM analysis was carried out using JSM-IT100 SEM produced by JEOL Corporation of Japan. To reduce the flow problem of modified asphalt caused by emission ion beam absorption, the accelerated voltage in SEM detection is 5 kV. In SEM analysis, different sizes of micro-topography were measured, including 100×, 200×, 500×, 1,000×, and 4,000×. The preparation process of the SEM test sample is as follows. The asphalt film sample was cut on the glass slide. Then, the glass slide was placed on a gold spraying test bench with conductive adhesive, and the surface was sprayed for 90 s. After the samples have electrical conductivity, they are put into the SEM test bed for testing.

#### 2.2.1.2 AFM analysis

The Dimension FastScan Scanning probe microscope produced by Bruker company was used to characterize the surface roughness change of UV aged modified asphalt. The scanning probe was used to scan the micro-morphology of the sample surface in ScanAsyst intelligent mode. The instrument probe was a silicon nitride cantilever probe. Checking view sizes of AFM test were selected as 80 μm × 80 μm and 30 μm × 30 μm.

### 2.2.2 Selection of detection area

To eliminate the influence of different locations on the results and reduce the subjectivity of the test results, we can reduce the randomness of HALS in asphalt through macro and micro means. At the macro scale, the dropper drops the asphalt modified by fluid HALS uniformly on the slide. After the asphalt is self-leveled and cooled to room temperature, conductive tape frame selects the detection area. The influence of randomness on the evaluation results is reduced by dividing the scanning area of the instrument, and the thickness of the four corners and center of each film are tested using the UV-Visible NIR-MSP film thickness meter. At the micro-scale, the microscopic scanning area is further divided (as shown in Figure 2(c)), and five regions, upper left, upper right, middle, lower left, and lower right, are selected to select the microscopic topography of samples accurately. The microscopic topography in each area is evaluated. The weighted average score is obtained by combining the thickness test data to get the final evaluation result.

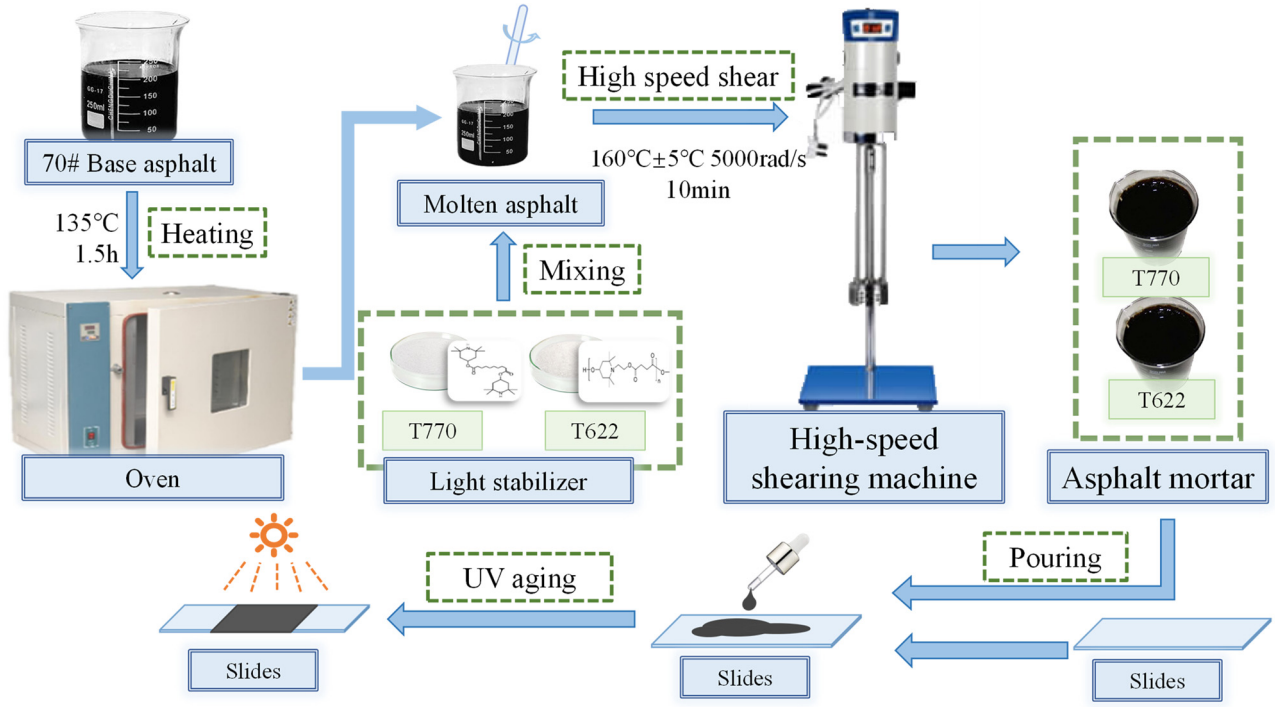


**Figure 1:** Light stabilizer modified asphalt preparation process.

#### 2.2.3 Evaluation method

To evaluate the evolution process of asphalt aging, SEM and AFM detection techniques were used to assess the aging stage of asphalt. By defining and quantifying the unique structure of the asphalt aging process, we classify the degree of aging at each location. Based on the joint action of SEM and AFM evaluation methods, the influence of UV radiation on the advanced state of asphalt was evaluated using the crack characteristics and asphaltene content variation characteristics in the aging process of asphalt. Combined with the percentage of specific structure area and roughness parameters determined by the AFM evaluation method, relevant parameters can be set to evaluate the short aging of asphalt materials. As the evaluation parameters in this study have few limiting factors, the method can be further used to verify the aging effect of anti-aging materials at various stages. The process is shown in Figure 3.

# 3 Results and discussion

## 3.1 Characterization of UV-induced micro-morphology evolution behavior based on SEM analysis

### 3.1.1 UV-induced micro-structure evolution of asphalt binder

#### 3.1.1.1 Base asphalt

Figure 4 shows the UV-induced micro-morphologies of the base asphalt with different scanning multiples. From Figure 4(a) (500 μm) and Figure 4(b) (200 μm), the surface of the base asphalt showed a distinct aggregation of parallel-state cracks (marked in yellow) and a locally present closed-like fragmentation region (marked in red) after UV aging at 76.25 h. When the crack was magnified 500× (Figure 4(c)), it was found that the middle part of the fracture was

**Table 2:** Relationship between outdoor and indoor aging time conversion

| Natural light time | 0 month | 3 months | 6 months | 9 months | 12 months |
|---|---|---|---|---|---|
| Simulate the lighting time | 0 h | 76.25 h | 152.5 h | 228 h | 305 h |

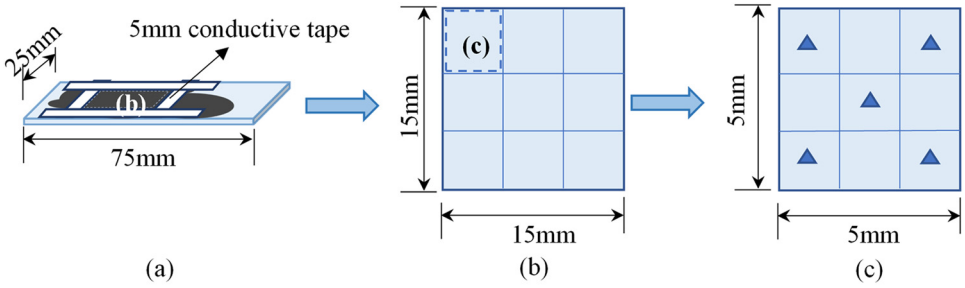


**Figure 2:** The selection process of the detection area. (a) Selection of scanning area, (b) macroscopic division of scanning area, and (c) microscopic division of scanning area.

straight, and the two ends were deflected at a certain angle. There is no trend of interconnection or direct connection between cracks. Further magnification of the fissures to 1,000× (Figure 4(d)) and 2,000× (Figure 4(e)) confirmed that there were no connections between the cracks, which all appeared in an independent form. When the UV aging time was extended to 152.5 h, a series of closed lumps appeared on the asphalt surface, and there was apparent

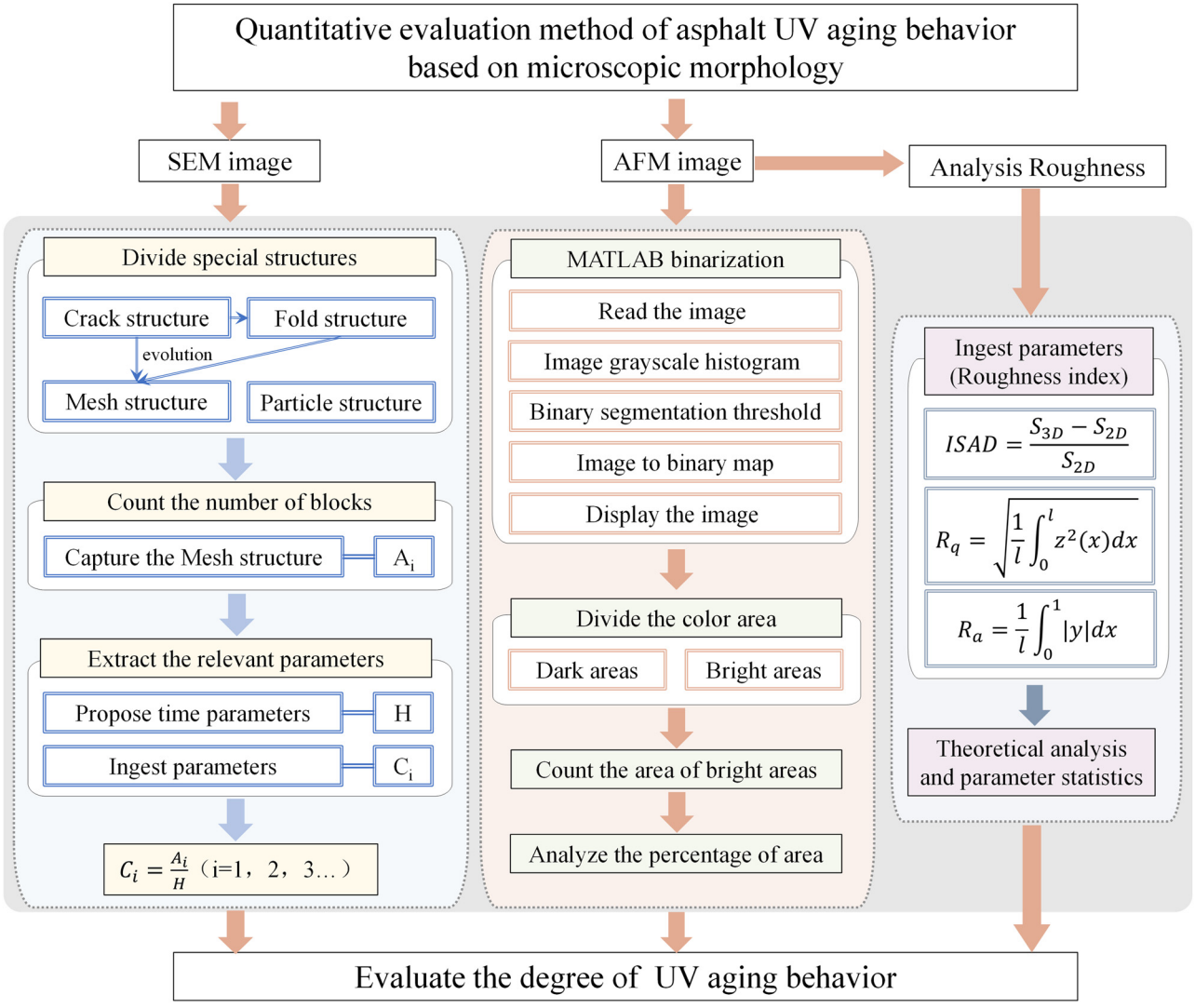


**Figure 3:** Evaluation of the aging process of asphalt after being affected by UV radiation.

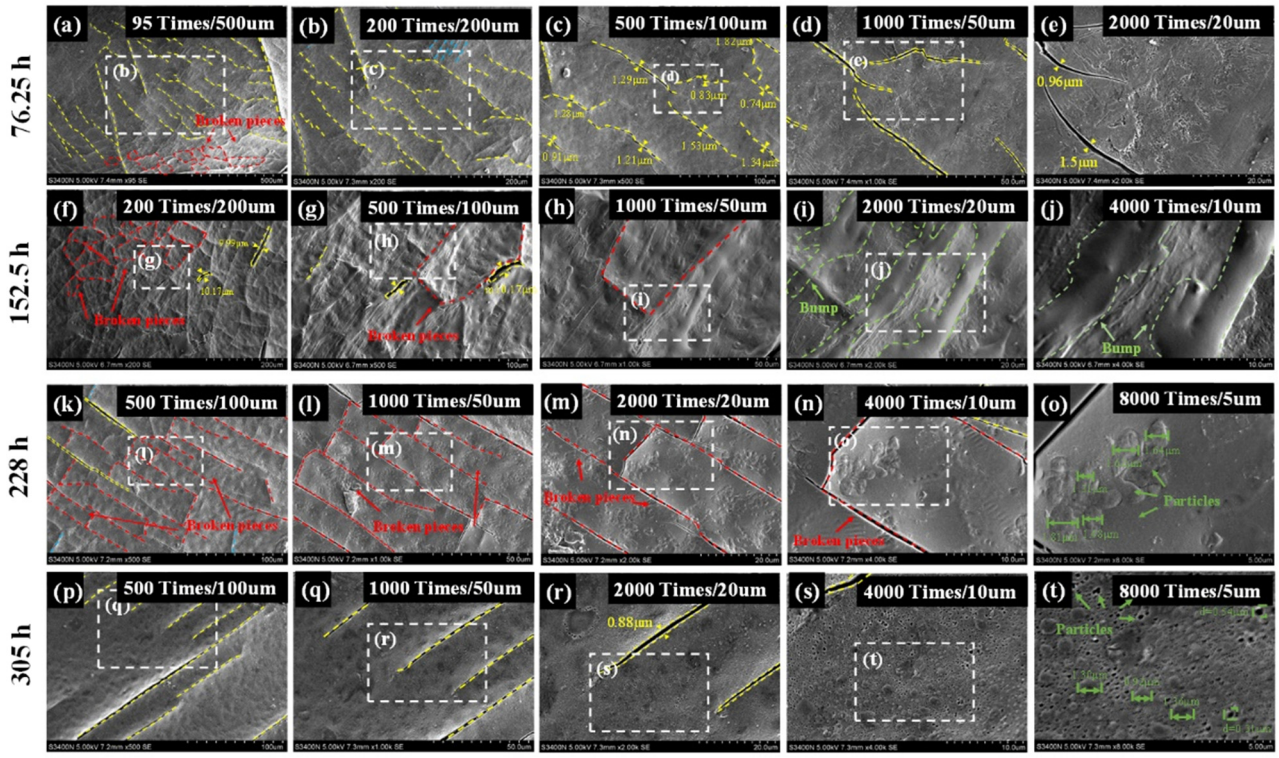


**Figure 4:** SEM morphology of base asphalt affected by UV aging. (a) 76.25 h–500 μm, (b) 76.25 h–200 μm, (c) 76.25 h–100 μm, (d) 76.25 h–50 μm, (e) 76.25 h–20 μm, (f) 152.5 h–200 μm, (g) 152.5 h–100 μm, (h) 152.5 h–50 μm, (i) 152.5 h–20 μm, (j) 152.5 h–10 μm, (k) 228 h–200 μm, (l) 228 h–100 μm, (m) 228 h–50 μm, (n) 228 h–10 μm, (o) 228 h–5 μm, (p) 305 h–100 μm, (q) 305 h–50 μm, (r) 305 h–20 μm, (s) 305 h–10 μm, and (t) 305 h–5 μm.

common boundary between the nodes, as can be observed in Figure 4(f). When the locally closed block was magnified (Figure 4(g)), it was shown that the league boundary was not a crack but a bulge. When the border was stretched further, the morphology of the protuberant structure could be observed clearly. The bulge structure was a strip structure higher than the surrounding flat area. This convex structure was very similar to the crack appearance at 76.25 h, which may be caused by the increase in the temperature of asphalt after absorbing UV radiation, and the formation of bulge structure after filling the crack position.

When the UV aging time reaches 228 h (Figure 4(k)), it can be observed that more dense parallel cracks appear again on the asphalt surface. Compared with 76.25 h, after 228 h UV aging, vertical cracks appear that intersect with parallel cracks on the asphalt surface. Vertical fractures connected the original parallel fractures and led to the appearance of closed fractures and massive fragments. When the local fractures were placed between 1,000 and 2,000× (Figure 4(l) and (m)), it was found that there were vertical fracture connections between different parallel fractures. There were obvious closed cracks in this stage, mostly rectangle-like structures. After further magnification of the rectangular frame (Figure 4(n) and (o)), a circular bulge structure with a diameter of about 1.5 μm was identified within it. The results of UV aging at 305 h are shown in Figure 4(p)–(r). It can be seen that the closed cracks on the asphalt surface disappear, parallel cracks appear, and the density and number of cracks decrease significantly. Local magnification of the fracture to 4,000- and 8,000-fold (Figure 4(s) and (t)) revealed a rounded bulge structure and holes of different diameters in the region around the fracture.

In summary, micro-crack was the main characteristic structure of morphology evolution in the micro-morphology change induced by UV, and there was a certain regularity in its transformation. The statistical analysis of the typical parameters of the cracks in the visual field was carried out based on the microscopic features. After 75.25 h UV aging, the crack width range of the base asphalt surface was 0.74–1.83 μm. After 152.5 h UV aging, the asphalt surface crack structure appeared at a certain degree of "healing." After 228 h, the cracks increase, and the width ranges from 0.26 to 0.60 μm. When the UV aging time reaches 305 h, the crack width ranges from 0.65 to 1.92 μm.

The appearance of a cracked structure is a sign that asphalt has entered the aging stage. Based on the analysis of Figure 4 and its characteristic form, the fracture spacing

is selected as an evaluation index to predict the aging process of asphalt, and its corresponding parameters have the potential to be used as quantitative standard indexes. As seen from the Figure, surface cracks can be considered disjoint (parallel) independent existence in the early stage of asphalt aging. With the increase in aging degree, the number of fracture structures increases, and the maximum spacing between parallel fractures changes. It is inferred that UV aging affects the spacing of cracks on asphalt surfaces. Statistical analysis of the micro-morphology samples found that the spacing between different cracks (labeled examples in Figure 5) was significantly correlated with UV aging time. According to the statistical results of 200 samples (about 50 pictures at each aging time point) (Figure 5), the UV aging time was extended from 76.25 to 305 h. The spacing of fracture structure decreased from 42.86 to 26.42 μm. At the same time, the micro-structure characterization results were processed by ImageJ software, and it was found that most of the crack structures existed in a parallel state at a magnification of 1,000×. Compared with the microscopic morphology at 200×, the crack structures at 1,000× are sparse, and the overlap rate is low. It has favorable conditions for measuring the spacing of fracture structures.

#### 3.1.1.2 T770 light stabilizer modified asphalt

The UV-induced micro-morphology of T770-modified asphalt is shown in Figure 6. After UV aging for 76.25 h, micro-cracks with high density appeared on the surface of T770-modified asphalt. After magnification to 500× and 1,000× (Figure 6(b) and (c)), it can be seen that cracks are connected to form closed fragments with shallow cracking degrees and broad spreading areas. When amplified to 2,000× (Figure 6(d) and (e)), it is observed that the shape of the closed fragment is irregular, the width of the cracks at the boundary is large, and the surface of the piece is relatively flat. The cracks of T770-modified asphalt in the early aging stage float on the surface and do not cause deep aging. The UV aging time was further extended to 152.5 h, and the network structure composed of closed fragments could still be recognized on the surface of T770-modified asphalt. After further magnification to 500× and 1,000× (Figure 6(h) and (i)), it can be seen that the boundaries of each closed fragment structure are blurred, and the cracks are replaced by protrusions, due to the fluidity brought by rising temperature, leading to the healing of asphalt cracks. When magnified 2,000× (Figure 6(j)), the asphalt surface is rugged, which is due to the distribution of particle structure on the surface, and the particle structure size range is about 3.22–9.16 μm. It is speculated that part of the particles of the T770 light stabilizer dispersed into complete melting and emerged on the surface of the asphalt film with the flow of asphalt at high temperature.

After UV aging for 228 h, the micro-structure of T770-modified asphalt changes again, the boundary fuzzy closed fragmentation structure disappears, the convex structure changes into an apparent fold structure, and the area between the folds has a good flatness. After magnification to 1,000 and 2,000× (Figure 6(m)–(o)), a certain amount of particle structure still exists in the smooth region between folds, and the particle size is similar to that of the particle structure appearing at 152.5 h. In Figure 6(n), the maximum diameter of the "particle structure" can reach 7.51 μm. This phenomenon indicates that the photo-stabilizer is not entirely dissolved in the asphalt at this stage, so the bulge can still be seen in the enlarged micro-topography. When UV aging time was extended to 305 h, the fold structure density increased, but no apparent closed micro-structure was formed. It shows that the damage degree of the modified asphalt aging is not high, and there is no sharp crack.

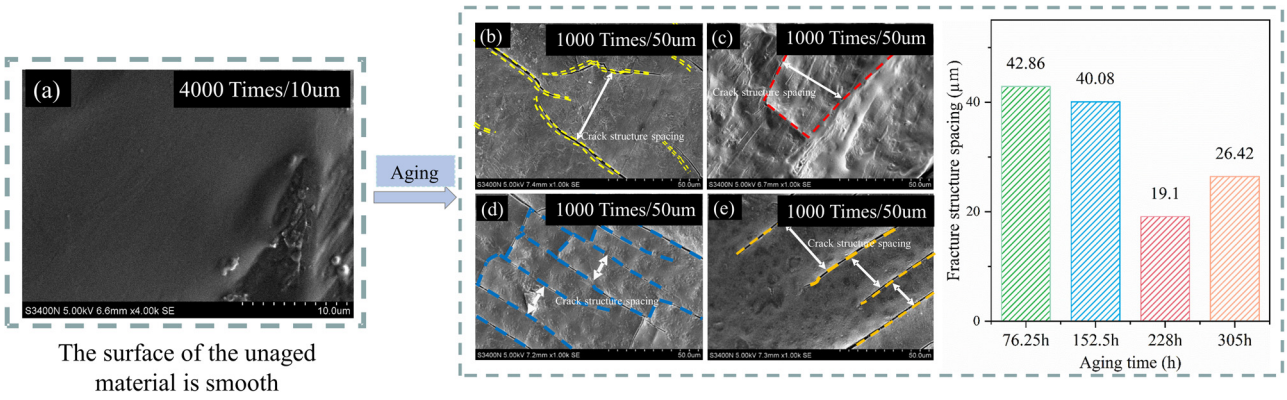


**Figure 5:** The spacing of base asphalt crack structure and the variation in crack spacing with UV aging: (a) 0 h, (b) 76.25 h, (c) 152.5 h, (d) 228 h, and (e) 305 h.

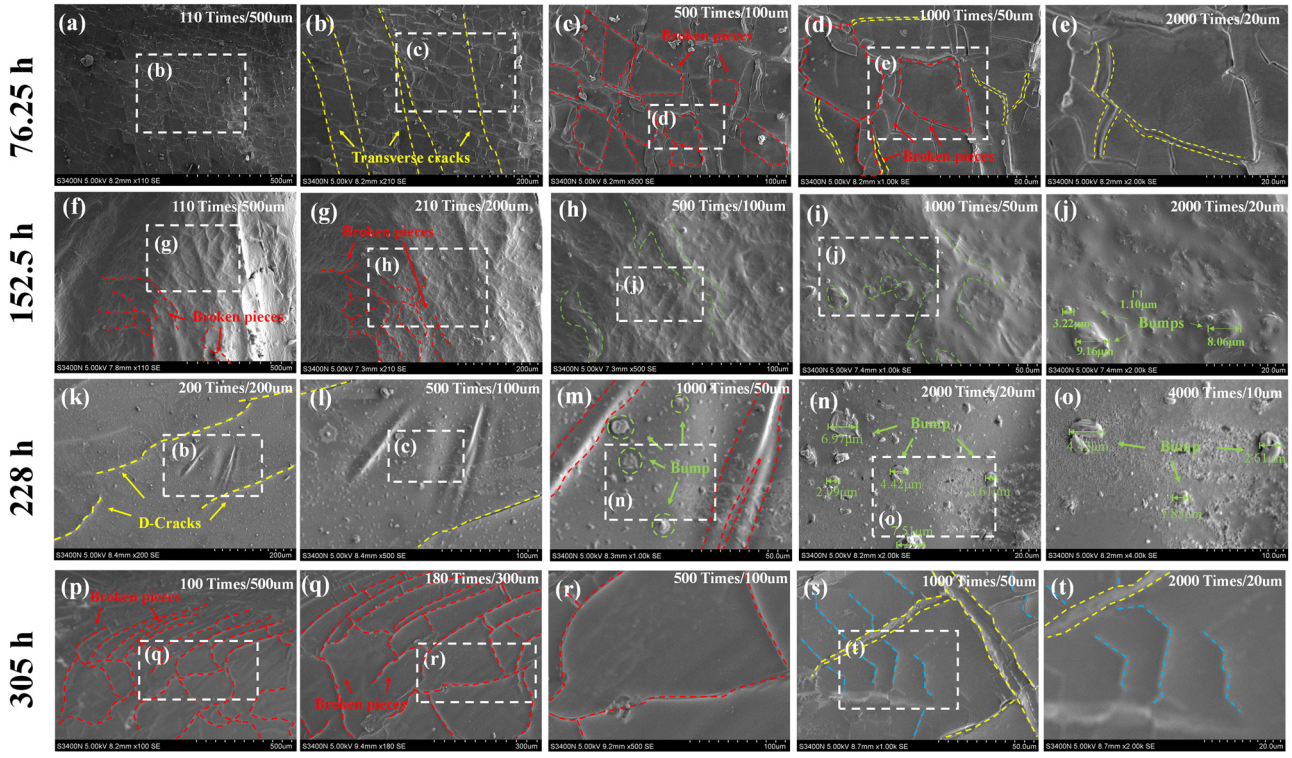


**Figure 6:** SEM morphology of T770-modified asphalt affected by UV aging. (a) 76.25 h–500 μm, (b) 76.25 h–200 μm, (c) 76.25 h–100 μm, (d) 76.25 h–50 μm, (e) 76.25 h–20 μm, (f) 152.5 h–500 μm, (g) 152.5 h–200 μm, (h) 152.5 h–100 μm, (i) 152.5 h–50 μm, (j) 152.5 h–20 μm, (k) 228 h–200 μm, (l) 228 h–100 μm, (m) 228 h–50 μm, (n) 228 h–20 μm, (o) 228 h–10 μm, (p) 305 h–500 μm, (q) 305 h–100 μm, (r) 305 h–100 μm, (s) 305 h–50 μm, and (t) 305 h–2 μm.

In conclusion, the crack structure of T770-modified asphalt appears in the early stage of UV aging and then evolves into a fold structure under the influence of UV radiation. With the deepening of the UV aging process, the density of the fold structure increases and lasts for a long time, which may be because T770 HALS delays the UV aging process of asphalt, improves the stability of asphalt colloidal structure, and then inhibits the further aging of asphalt. In the 152.5 h stage, most of the cracks in the asphalt micro-structure have intersections, which does not meet the definition of the crack structure. After UV aging for 305 h, the fold structure on the asphalt surface was connected to a closed network. This phenomenon may be because the UV aging effect of T770-modified asphalt is mainly concentrated on the surface, and its radiation effect has not penetrated the internal structure of the asphalt.

However, the folding structure is formed by the evolution of fracture structure, and the bulge formed when the asphalt was heated flowed, and covered. The spacing of cracks mainly determines the spacing of the fold structure. Therefore, based on the definition of fracture structure, the fold structure is defined as the fracture structure with the tendency to heal. Thus, the “unbonded” fold structure can still be selected to measure the maximum spacing, and its relevant parameters can still be as the standard index for quantifying T770-modified asphalt.

Based on Figure 6 and the analysis of characteristic structure, the micro-morphology samples were analyzed statistically. The distance between different folds (Figure 7) significantly correlates with UV aging time. Based on a sample size of 200 (approximately 50 pictures per aging time point), after 305 h UV aging, the wrinkle spacing of asphalt surface increased from 44.96 to 62.3 μm. At this time, the overlap ratio of fold structure was low, and the uplift in the middle of fold was apparent.

#### 3.1.1.3 T622 modified asphalt

Figure 8 shows the UV induced morphology of T622 modified asphalt. As shown in Figure 8(a) (200 μm), a valley-shaped “fold structure” appears on the surface of the asphalt after aging for 76.25 h, and the micro-structure of the asphalt is concave in the middle and convex in the periphery (marked with yellow). The width of the structure ranges from 9.21 to 33.51 μm. At 2,000 magnification (Figure 8(d)), irregular bulges exist between fold structures. Figure 8(f)

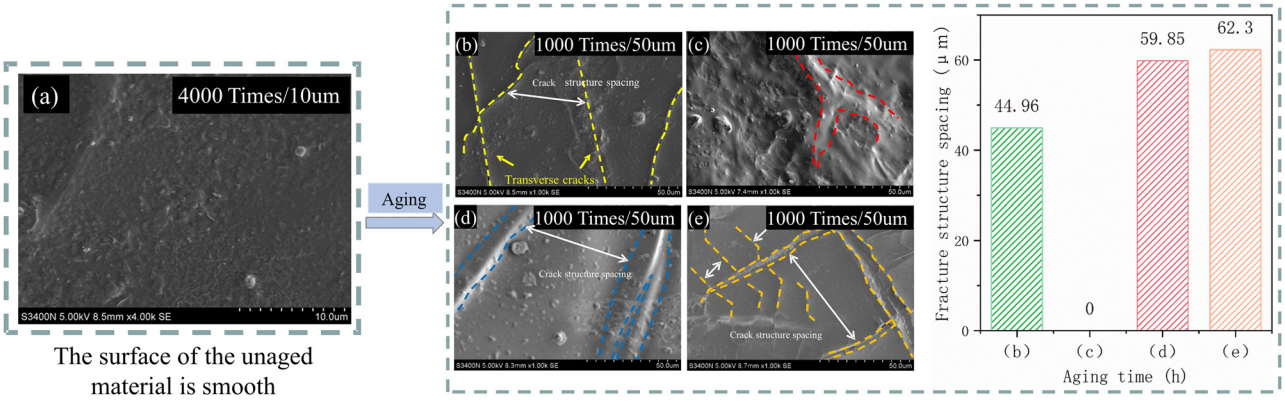


**Figure 7:** The spacing of T770-modified asphalt crack structure and the variation in crack spacing with UV aging: (a) 0 h, (b) 76.25 h, (c) 152.5 h, (d) 228 h, and (e) 305 h.

(200 μm) shows that the fold structures are more closely related and converge in the same direction. Further magnified to 2,000× and 4,000× (Figure 8(i) and (j)), the "raised" area forms a whole through interlacing, and the boundary with the fold structure becomes increasingly blurred. This may be because the asphalt was exposed to UV radiation and flowed in the high-temperature environment, filling the place of lightweight components lost during early aging. When UV aging time is extended to 228 h, it can be seen from the analysis of Figure 8(n) and (o) that the fracture structure initially formed on the asphalt surface transforms into an elongated "ridge" structure similar to the fold structure, and then gradually evolves into a tightly connected fold structure. This may be because, under continuous UV aging, the surface cracks appear briefly and then are covered with the traces left by the asphalt. Therefore, the

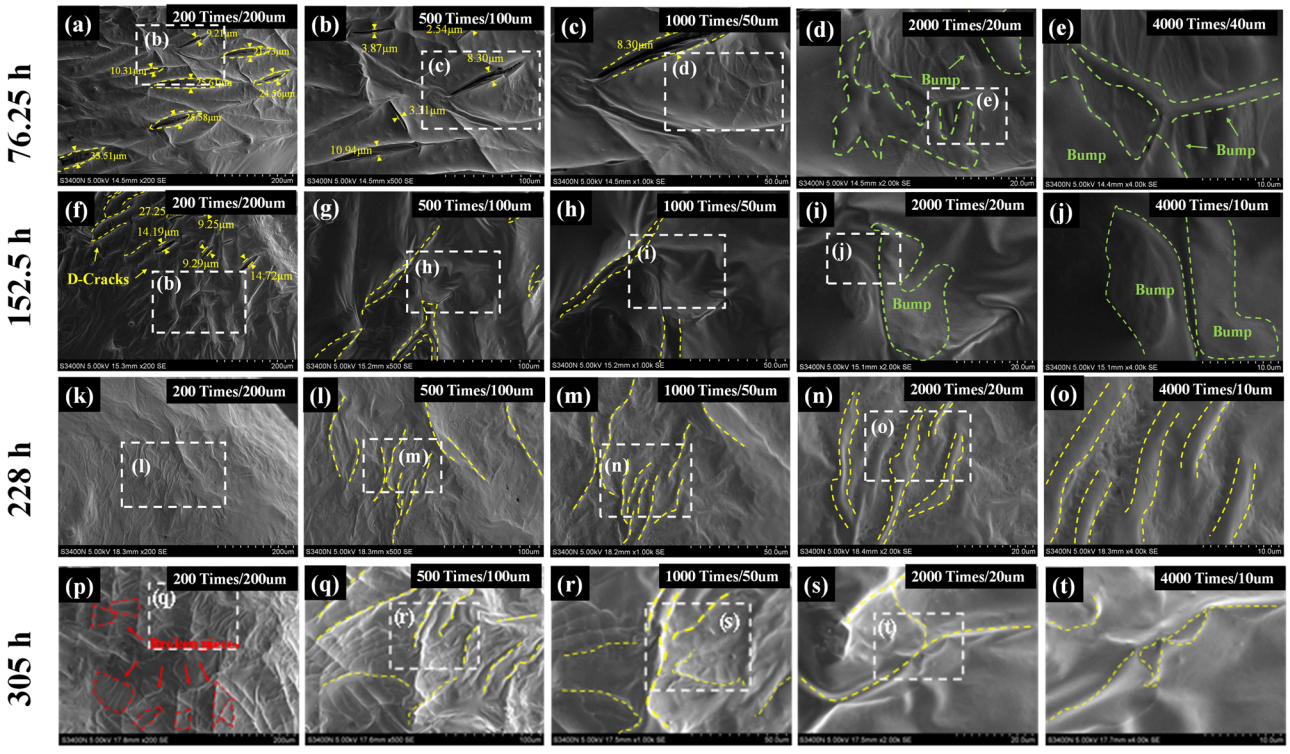


**Figure 8:** SEM morphology of T622-modified asphalt affected by UV aging. (a) 76.25 h–200 μm, (b) 76.25 h–100 μm, (c) 76.25 h–500 μm, (d) 76.25 h–20 μm, (e) 76.25 h–40 μm, (f) 152.5 h–200 μm, (g) 152.5 h–100 μm, (h) 152.5 h–50 μm, (i) 152.5 h–20 μm, (j) 152.5 h–10 μm, (k) 228 h–200 μm, (l) 228 h–100 μm, (m) 228 h–50 μm, (n) 228 h–20 μm, (o) 228 h–10 μm, (p) 305 h–200 μm, (q) 305 h–100 μm, (r) 305 h–50 μm, (s) 305 h–20 μm, and (t) 305 h–10 μm.

microscopic fold structure will show a parallel state. After UV aging for 305 h (Figure 8(p)), the morphology changes again, from the original parallel "fold structure" to a potentially staggered "network" structure. The structure is irregular and massive, but the smooth area between the systems becomes more extensive, with no obvious crack boundary. This indicates that the influence of UV aging on asphalt surface morphology is more prominent, forming a potential massive cataclastic area. Further magnification of local observation (Figure 8(s) and (t)) shows that the structural interface becomes more and more blurred with the extension of aging time, and the two are closely related.

As shown in Figure 9, the most prominent evolution process in the micro-area of T622-modified asphalt surface was "fold structure." SEM observed the development and formation of different fractures, and the change process of the distance between folds was studied for example, Figure 9. The edge of "fold structure" was evident, as shown in Figure 9(a), the width of "fold structure" was 36.55 μm. However, as the aging process deepens, the crack width becomes smaller, and the edge of the structure becomes more blurred.

The appearance of fold structure in asphalt microstructure may be caused by the flow of asphalt under the influence of high temperature and the filling of cracks, and the addition of T622 light stabilizer may enhance the self-healing ability of asphalt. It is inferred that the anti-aging performance of T622-modified asphalt under UV radiation might come from the self-healing performance of light stabilizer-modified asphalt and then promote crack healing to reach the anti-aging ability of UV radiation.

Based on the definition of crack structure and fold structure, the parameters related to "Crack structure" of T622-modified asphalt were selected as the quantitative standard indexes for the UV-induced typical micro-structure. Figure 9 shows that the crack interval of asphalt decreases from 36.55 to about 15.37 μm with aging time under long-term UV radiation. Comparing the crack spacing caused by UV aging of asphalt base under the same condition shows that both T622-modified asphalt and asphalt base tends to have more crack structures with aging. It was further demonstrated that T622-modified asphalt has anti-aging performance, but mainly to promote the asphalt by aging after the healing of cracks.

#### 3.1.1.4 Analysis of the evolution process of UV induced micro-morphology of modified asphalt

As shown in Figure 10, base asphalt, T770-modified asphalt, and T622-modified asphalt exhibit different evolution processes and characteristics after exposure to UV radiation. Based on the results of SEM analysis, the evolution process of base asphalt and T622-modified asphalt was similar. After 75.25 h of aging, a few cracks appeared on the surface of the two asphalt samples. When the UV aging time reaches 152.5 h, the micro-cracks on the surface of the base asphalt expand and densify, while the T622 modified asphalt shows this trend in the folded state. When the UV aging time was extended to 228 h, the crack on the surface of the asphalt base further expanded and closed, and the connecting and connecting position appeared to obviously fragmentate. At this time, T622-modified asphalt shows a similar development trend, but because of its anti-UV aging effect, the surface of T622-modified asphalt only appears through the fold, and there was no obvious fragmentation. When the UV aging time reaches 305 h, the micro-cracks on the surface of the base asphalt intersect with each other; the surface appears as closed debris and the boundary of the debris area warps. However, with the prolonged UV aging time, the surface wrinkle structure of T622-modified

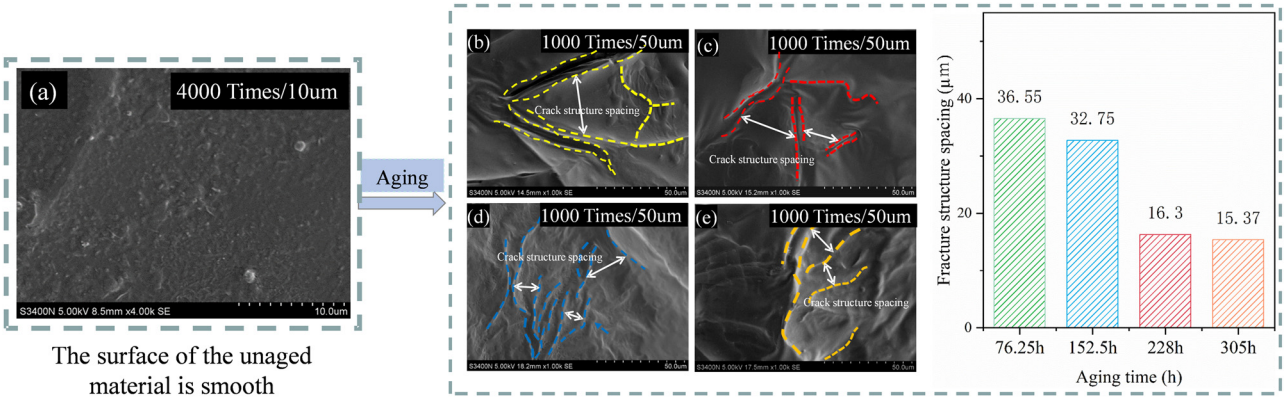


**Figure 9:** The spacing of T622 modified asphalt crack structure and the variation in crack spacing with UV aging: (a) 0 h, (b) 76.25 h, (c) 152.5 h, (d) 228 h, and (e) 305 h.

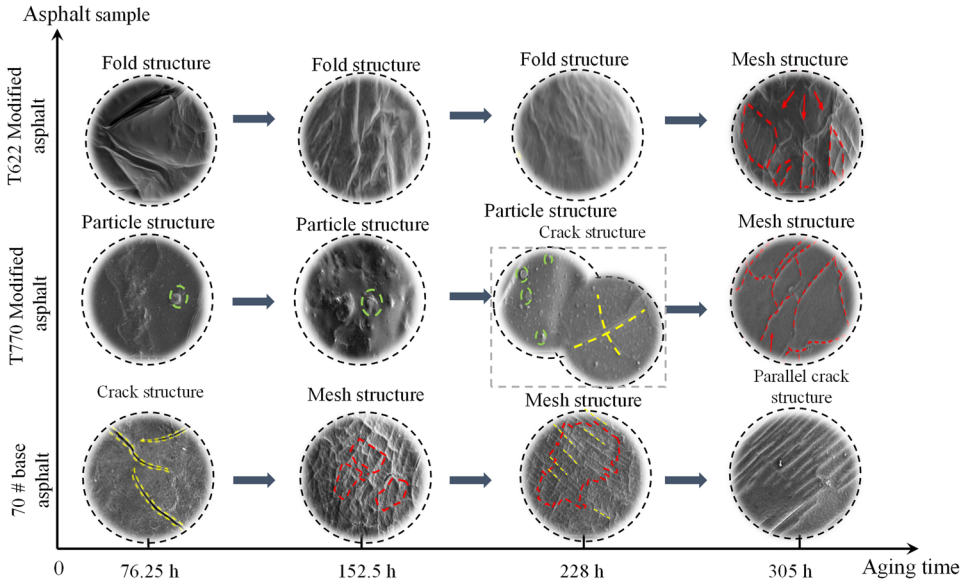


**Figure 10:** UV aging evolution of different asphalt specimens.

asphalt becomes denser, and the breakthrough boundary structure appears.

To sum up, the characteristic structure of base asphalt as the control group is "crack structure." The typical evolution process of micro-morphology was: "staggered crack structure" – "through network structure" – "parallel crack structure." The typical micro-structure of T622-modified asphalt is "fold structure," and the evolution process of typical morphology is "fold structure" – "network fold structure." The slow evolution of T770-modified asphalt may be due to the retarding effect of T770 on the aging of asphalt by retarded amine HALS. T770 light stabilizer improves the anti-aging performance of asphalt and prolongs the duration of each aging stage, which provides more abundant time for asphalt self-healing and thus delays the UV aging process. However, the number of "crack structures" of T770-modified asphalt at the same aging time was less. The typical evolution process of micro-morphology of T770 light stabilizer modified asphalt is "grain structure" – "crack structure" – "network structure."

The results show that the crack width of asphalt base was large, and the degree of crack penetration and propagation was more serious than that of light-stabilized asphalt. For T770- modified asphalt, the evolution process of "crack structure" was slower, which shows that T770 light stabilizer can delay the change in morphology induced by UV in the micro-layer. For T622-modified asphalt, the interval width of the "fold structure" was used to characterize and describe the UV aging characteristics of asphalt. Under the influence of long-term UV radiation, the aging process of different types of asphalt will eventually show the same "network structure." The addition of T770 and T622 can delay the change in asphalt micro-morphology.

### 3.1.2 Typical structure classification and definition of asphalt UV aging micro-morphology determination

At the early stage of UV aging, the typical micro-structure of asphalt surface is "crack structure" (Figure 11(a)–(c)). The crack structure presents a linear extension distribution, different cracks often exist independently. The crack width decreases gradually from the middle to the two ends, and the ends will appear in arc deformation direction, and the bituminous surface between the cracks was relatively smooth. Under the influence of UV aging, the cracks appear gradually on the original smooth asphalt surface. Although they have not extended to the internal structure, the appearance of cracks will lead to rapid aging of asphalt materials in a short time. Eventually, the cracks spread out and formed a "mesh."

The "network structure" shown in Figure 11(d)–(f) was the main typical structure form of asphalt in the late UV aging stage. The network structure mainly consists of staggered cracks formed through extension, connection, and penetration. The typical reticular structure has a relatively normal formation process. In the early stage of the structure, the area was large, and the boundary was not obvious. As the number of cracks increases, the area of the network structure becomes small, and the boundary becomes clear.

Finally, the asphalt surface was divided by cracks into independent fragments of relatively regular size and shape. The comparative analysis of the samples' structural characteristics shows that stable "network structure" can be used as an indicator to distinguish the aging stage of asphalt. The fundamental reason was that there was a valuable point for the formation of network structure – when the aging of asphalt exceeds the range of self-healing ability of asphalt, the stable network structure appears. The later the network structure appears, the stronger the asphalt can withstand the effects of aging. Therefore, the typical micro-structure "network structure" can be used as an essential basis to judge the UV aging degree of asphalt.

"Fold structure" is mainly shown in Figure 11(j)–(l), which exists in multiple aging stages. Under UV radiation, the asphalt surface temperature rises, which promotes the asphalt itself to self-healing, and the spontaneous flow fills the cracks on the asphalt surface, thus forming a special fold structure [24,25]. Based on this, the fold structure was selected as one of the typical discriminant structures of UV aging micro-structure, which can be used to define and distinguish the intermediate stage between the early and late UV aging of asphalt. However, the limited self-healing ability of asphalt does not contribute much for the resistance to the generation and expansion of asphalt pavement cracks, the essence of which lies in the fact that the self-healing ability of asphalt cannot eliminate the influence of UV aging on asphalt materials [25].

"Particle structure" (Figure 11(g)–(i)), as another type of characteristic structure, mainly appears on the relatively flat asphalt surface between cracks, folds, reticular structures, and other structures. According to the particle

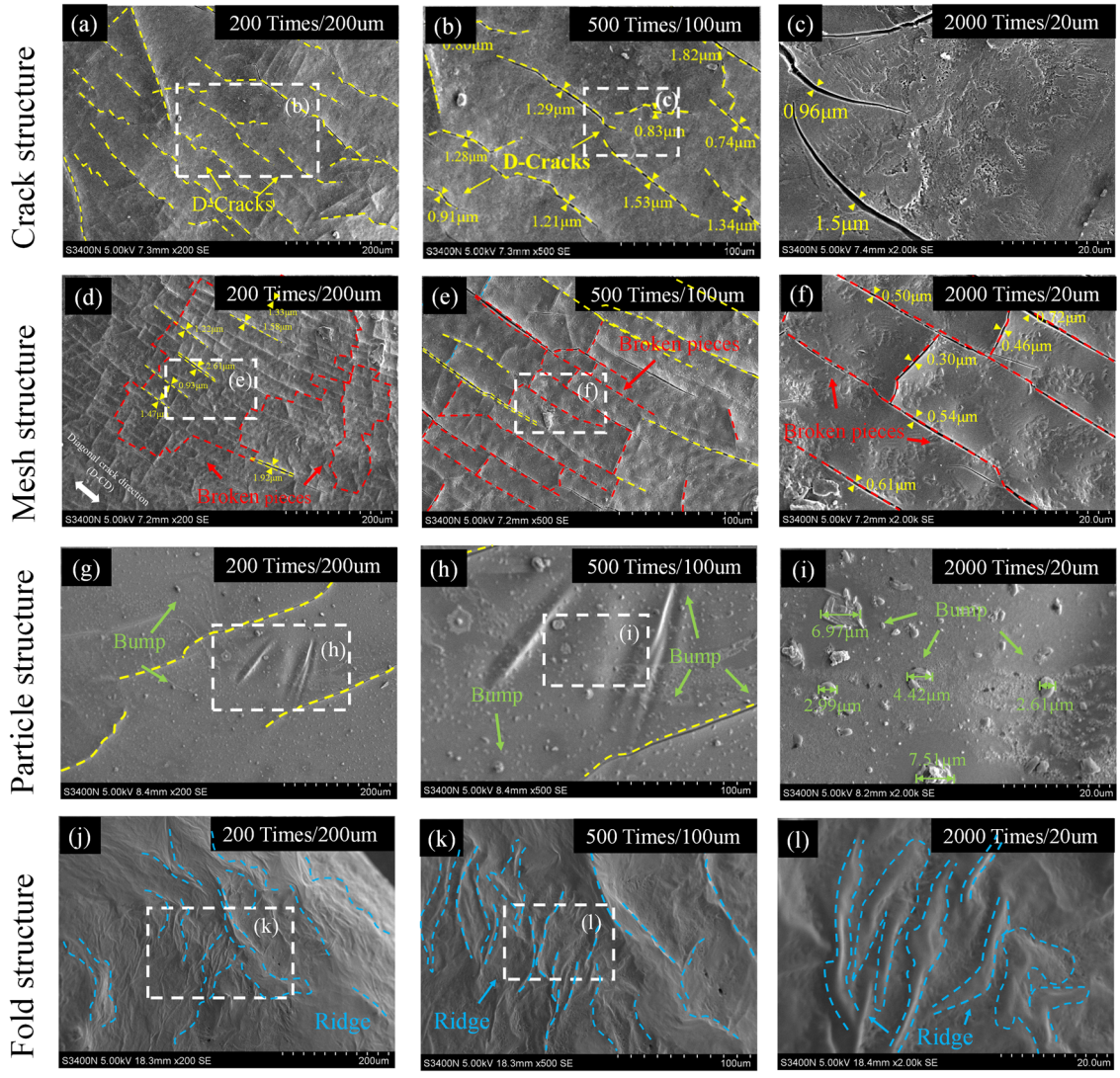


**Figure 11:** Typical characteristic structure of micro-morphological evolution of asphalt UV aging. (a)–(c) Crack structure, (d)–(f) Fold structure, (g)–(i) Particle structure, and (j)–(l) Mesh structure.

structure and its morphological characteristics in different samples, it can be inferred that there were two main reasons for the formation of particle structure.

(1) After the crack or fold structure appears, the surface tension of asphalt will change significantly, resulting in a slight bulge and uplift in some areas and finally forming a granular structure.
(2) Some small particles of HALS were embedded in asphalt material during the preparation of asphalt film by dissolution evaporation after the HALS melts into asphalt. With UV aging, some areas of the asphalt surface appear to soften and flow, and the embedded HALS particles were gradually exposed, thus forming a granular structure.

In summary, observing the microscopic morphology of asphalt under UV radiation shows that the formation reasons of different types of characteristic structures are different and have certain regularity. Cracks begin to appear in the early stages of aging. As asphalt is affected by external aging, its microscopic surface may form a granular structure due to incomplete melting of modifiers or fold structure due to the flow of asphalt. However, under the action of long-term UV aging, the crack structure will eventually develop into a network structure [23]. Thus, the emergence of the reticular structure can be considered a stage of aging.

### 3.1.3 Quantitative analysis of UV aging behavior of light stabilizer-modified asphalt based on microscopic morphology

The 200× SEM scanning results based on different UV aging times are shown in Figure 12. The microstructure of asphalt in UV aging process mainly includes crack structure, fold structure, and network structure. The formation of these three microstructures has a specific correlation. Among them, the network structure is formed after the continuous development and penetration of fracture structure. As a typical microstructure of asphalt in the early stage of UV aging, the crack structure's development and extension rate determines the network structure's emergence rate. Based on this, the network structure can reflect the development and degree of UV aging of asphalt. The density of individual fragments in the network structure can also be directly related to the fracture density. Therefore, the "network structure" was selected as the main basis for the micro-quantitative analysis of UV aging asphalt.

Based on the data in Table 3, the time nodes of the "network structure" of different types of asphalt were other, and the relevant parameters of quantitative analysis were extracted. The selection stage includes base asphalt-152.5 h, base asphalt-228 h, T770-modified asphalt-305 h, and T622-modified asphalt-305 h. The corresponding calculation formula (formula (1)) was used to calculate in detail the evaluation parameters of the characteristic structure as $C_i$ ($i$ = 1, 2, 3). Among them, the definition and calculation of preliminary evaluation parameters of network structure were mainly based on the following:

$$C_i = \frac{A_i}{H}, \quad (i = 1, 2, 3 \ldots), \tag{1}$$

where $C_i$ is the number of network structures appearing in the unit aging time, unit: block. $A_i$ is the existing number of network structures obtained statistically under the condition of constant total area, which are $A_1$ (base asphalt-152.5 h), $A_2$ (base asphalt-228 h), $A_3$ (T770-modified asphalt-305 h), and $A_4$ (T622-modified asphalt-305 h), unit: block (as illustrated in Figure 13). $H$ is the UV aging time corresponding to different stages, unit: hours.

#### 3.1.3.1 Time parameter introduction

Generally, asphalt "network structure" has a more apparent aging degree. As can be seen from Table 4, ImageJ image processing means were used to reprocess the SEM topography, count the number of "network structures," and obtain the following results: $A_2 > A_4 > A_1 > A_3$. Based on this, it can be seen that base asphalt has the most significant number of Network structures in unit time at 228 h, followed by T622-modified asphalt at 305 h and base asphalt at 152.5 h. After comparison, it can be judged that after 305 h aging, T770-modified asphalt was in the aged stage of base asphalt 152.5 h, and after 305 h aging, T622-modified asphalt was in the aging location of base asphalt 152.5–228 h. To further quantify the microscopic evolution process of asphalt under the influence of UV radiation aging and the effect of HALS, the time parameter $H$ was introduced on this basis (as shown in formula (1)). It can be seen that the asphalt aging rate from large to small was $C_2 > C_1 > C_4 > C_3$ after the introduction of the time factor.

These results indicate that the base asphalt has encountered a severe UV aging effect in the 228 h stage, resulting in a surge in the number of microscopic "network structures" of asphalt per unit. In contrast, the aging rate of base asphalt at the 152.5 h stage was $C_1$ = 0.494 pieces per h, indicating that the aging process was faster with the extension of aging time. The aging rate of T770-modified asphalt was $C_3$ = 0.043 pieces per h, which was only 0.067% of the aging rate of base asphalt in the 305 h stage and better than the aging rate of T622-modified asphalt $C_4$ = 0.268 pieces per h.

Under the same aging condition, the modified asphalt with HALS enters the next aged stage later than the base

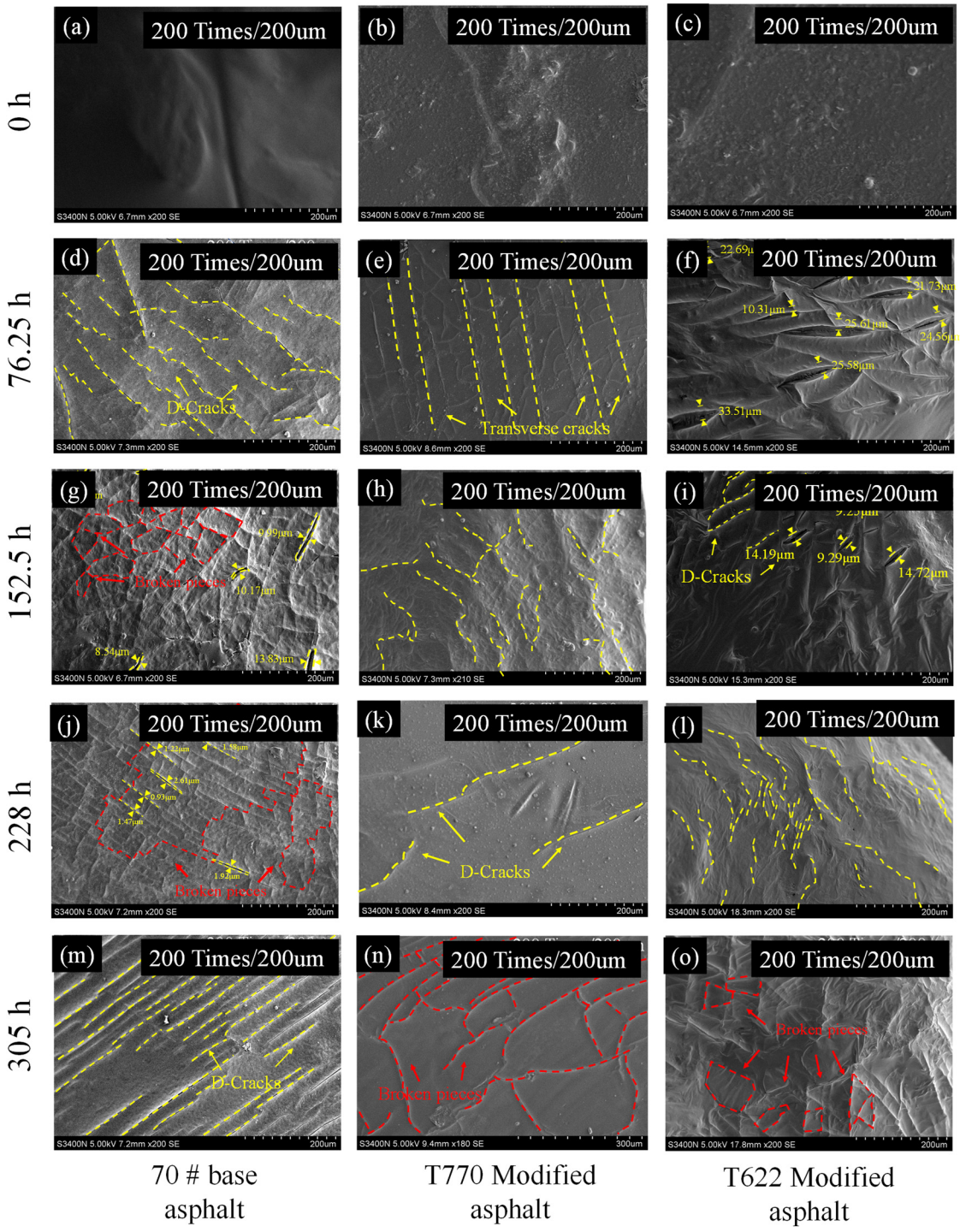


**Figure 12:** Typical microscopic morphology of asphalt under different UV aging times. (a) 70 # Base asphalt-0 h, (b) T770-modified asphalt-0 h, (c) T622-modified asphalt-0 h, (d) 70 # base asphalt-76.25 h, (e) T770-modified asphalt -76.25h, (f) T622-modified asphalt -76.25h, (g) 70 # asphalt base -152.5h, (h) T770-modified asphalt -152.5h, (i) T622-modified Bitumen - 152.5h, (j) 70 # base bitumen - 228 h, (k) T770-modified Asphalt -228 h, (l) T622-modified asphalt -228 h, (m) 70 # Asphalt base -305 h, (n) T770-modified Asphalt -305 h, and (o) T622-modified asphalt -305 h.

asphalt. Therefore, the microscopic damage degree of T770- and T622- modified asphalt is much lower than that of base asphalt at the same aging stage. It can be further explained that HALS has good anti-aging properties. In particular, the T770 light stabilizer can effectively reduce the aging rate of asphalt.

**Table 3:** Typical structural occurrence nodes of different types of asphalt after UV aging

| Asphalt type | 0 h | 76.25 h | 152.5 h | 228 h | 305 h |
|---|---|---|---|---|---|
| Base asphalt | Flat surface | Crack structure | Network structure | Network structure | Crack structure |
| T770-modified asphalt | Flat surface | Particle structure | Particle structure | Crack/particle structure | Network structure |
| T622-modified asphalt | Flat surface | Fold structure | Fold structure | Fold structure | Network structure |

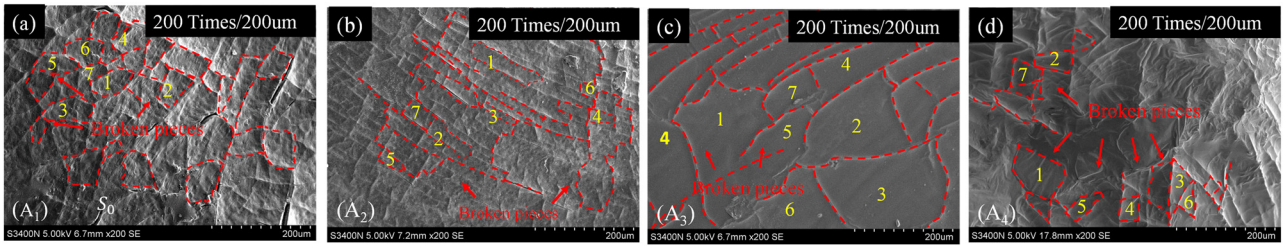


**Figure 13:** The selection of network structure areas: (a) $A_1$-152.5 h, (b) $A_2$-228 h, (c) $A_3$-305 h, and (d) $A_4$-305 h.

In Table 4, $S_0$ is the area of SEM view field under magnification. Under the condition that the total size of the statistical block $A_i$ is unchanged, the existence number of the network structure are obtained statistically, which are $A_1$ (base asphalt-152.5 h), $A_2$ (base asphalt-228 h), $A_3$ (T770-modified asphalt-305 h), and $A_4$ (T622-modified asphalt-305 h), unit: block, as demonstrated in Figure 13. $H$ is the corresponding UV aging time of different stages, unit: hours (h). The parameter $C_i$ is the number of occurrences of the network structure in the unit aging time, unit: block.

### 3.1.3.2 Introduction of feature structure parameters

The above research methods and parameters were mainly based on the stable "network structure" after a long time of aging. However, the micro-structure changes of asphalt in UV aging were very complicated. When two or more characteristic structures (network structure and crack structure or fold structure) exist simultaneously, certain correction treatment was needed to improve the accuracy of analysis results. Therefore, correction coefficients were set in this work for UV aging stages with various typical characteristic structures (Table 5), as shown below.

$$C_i = A_i \times x_i. \tag{2}$$

where the parameter $C_i$ is the number of occurrences of the network structure in the unit aging time, unit: block; Statistical number of blocks $A_i$ is the number of network structures obtained under the condition that the total area is unchanged, unit: block; It is the correction factor of the UV aging stage of a variety of typical characteristic structures. As demonstrated in Section 3.1.2, there were four characteristic structures (network structure, fold structure, particle structure, and crack structure) after UV aging. The characteristics of typical distinct structures were quantified, and the asphalt aging process was described. The quantitative analysis of the UV aging results of base asphalt showed that only the "network structure" existed in the aging stage of base asphalt-152.5 h. With the asphalt aging

**Table 5:** Deviation correction coefficients

| Parameter | Deviation correction value $x_i$ |
|---|---|
| Same structure | 1 |
| Two or more structures | 1.2 |

**Table 4:** Quantification of the aging process of asphalt reticular structure at different times

| Parameter | Base asphalt-152.5 h | Base asphalt-228 h | T770-305 h | T622-305 h |
|---|---|---|---|---|
| Total area $S_0$ | | 280,000 μm$^2$ | | |
| Count of the number of blocks $A_i$/block | 75 | 146 | 13 | 82 |
| Aging time $H$ | 152.5 | 228 | 305 | 305 |
| Parameter $C_i$/block $h^1$ | 0.494 | 0.641 | 0.043 | 0.268 |

**Table 6:** Quantitative correction of aging process of asphalt network structure at different times

| Parameter | Base asphalt-152.5 h | Base asphalt-228 h | T770-305 h | T622-305 h |
|---|---|---|---|---|
| Count of the number of blocks $A_i$/block | 75. | 146 | 13. | 82 |
| Parameter correction $B_i$ | 75 | 175 | 16 | 82 |
| Parameter $C_i$ | 0.494 | 0.769 | 0.052 | 0.268 |

**Table 7:** Asphalt aging process rates at different times

| Aging rate | 76.25 h | 152.5 h | 228 h | 305 h |
|---|---|---|---|---|
| Base asphalt | 0.317 | 0.494 | 0.769 | 1.197 |
| T770-modified asphalt | 0.014 | 0.021 | 0.033 | 0.052 |
| T622-modified asphalt | 0.071 | 0.111 | 0.172 | 0.268 |

time advancing to 228 h, the "network structure" and parallel "crack structure" coexist in the surface micro-structure results of the base asphalt. At this time, different types of characteristic structural parameters were transformed into a unified structure for evaluation.

It was assumed that there were various characteristic structures when asphalt was aged in UV. Under the condition that the total area was unchanged, the deviation correction parameter (Table 5) was introduced into the existing number $A_i$ of the statistically obtained network structure as the actual number of blocks $B_i$ (Table 6). The aging rate parameter $C_i$ was corrected again with the introduction of the characteristic structure parameters, and the results are shown in Table 7.

To sum up, it can be concluded that the time stage and duration of the "network structure" of different asphalt samples are different. The "network structure" stage of 70# base asphalt is the earliest, and the "network structure" stage of modified asphalt is later. This indicates that the aging degree of modified asphalt is lower in the same aging time stage. Further analysis shows that the aging rates of different asphalt samples are significantly different even at the same aging stage. The aging rate of T770-modified asphalt is the slowest in each UV aging stage, followed by T622 modified asphalt, which indicates that the anti-aging ability of T770 subjected to HALS is better than that of T622 subjected to HALS. Through the quantitative analysis of the characteristic structural changes in SEM characterization methods, it can be determined that the anti-aging ability in descending order is T770 > T622 > 70# base asphalt.

### 3.1.4 UV induced micro-morphology evolution behavior and typical structure analysis based on AFM

Based on AFM test, the microscopic evolution of asphalt samples under UV radiation was studied. The study of AFM two-dimensional (2D) topography image mainly shows in the area statistics of "bright field" structure. Common image analysis software includes Image-Pro Plus, ImageJ, and MATLAB. As shown in the Figure 14, an AFM image of unaged asphalt is selected as an example. Based on the maximum value method, the AFM 2D morphology was treated with grayscale. The gray image was binarized based on the im2bw function, and its threshold was selected as 0.5. Finally, Image-Pro Plus software was used for regional selection to output the bright field structure area in 2D graphics. In addition, for the study of AFM three-dimensional (3D) topography, Nanoscope Analysis 1.8 software can be used to obtain the relevant data on asphalt surface roughness.

The results show that the "bright field" in AFM-2D morphology increases with the aging time. Further analysis showed that the "bright domain" was mainly composed of gum, asphaltene, wax, and other substances [22–24]. It was inferred that with the increase in the special structure area ratio, asphaltene content increased, and the degree of aging increased. In addition, the variation in roughness in AFM-3D morphology can also prove that the asphalt samples are affected by UV radiation.

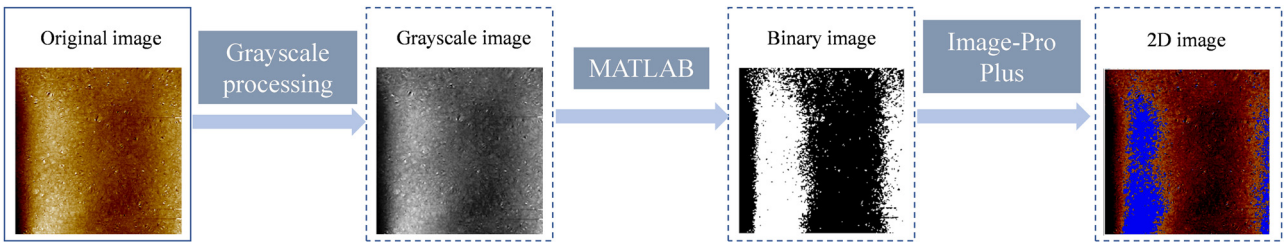


**Figure 14:** The processing method and area selection of bright domain structure in AFM-2D image.

In summary, the study on the evolution process of the micro-topography of AFM provides a basis for further statistics of the bright field structure area in the subsequent research.

### 3.1.5 Micro-morphological evolution of asphalt under different UV aging times

#### 3.1.5.1 Base asphalt

Figures 15 and 16 show base asphalt's AFM characterization results under different UV aging times. The unaged 70# base asphalt (Figure 15(a)) was analyzed, and it was found that the 2D topography of the base asphalt showed evident bright and dark regions, and the bright granular structure was evenly dispersed in the image. Through the observation of the roughness index, it is found that the highest value of the image is 21.1 nm, and the lowest value is −28.6 nm. Generally speaking, the asphalt surface tends to be flat on the whole.

However, according to the 3D analysis results (Figure 16(a)), the surface morphology of the unaged base asphalt was more prominent. It can be seen from the observation that the bright domain was manifested as a raised area, and the dark domain was manifested as a sagging area. When the UV aging time reaches 76.25 h, the overall morphology of asphalt in Figure 15(b) gradually becomes more complex, and the distribution of bright and dark domains presents obvious aggregation boundaries. The accumulation of materials on the asphalt surface forms bright domain aggregation, which was gradually reflected with increasing aging depth. At this aging stage, the surface of the base asphalt tends to flatten out, and the total height decreases, which was shown in the 3D topography map (Figure 16(b)) as evenly distributed "raised" and "sunken" areas. As the UV aging time continues to extend to 228 h (Figure 15(d)), the boundary between the bright domain and the dark domain becomes more apparent, and most of them take the bright domain as the core and spread around, and then connect into the form of the dark domain.

In addition, the 3D topography of this period (Figure 16(d)) presents a large-diameter aggregated "columnar structure." After 305 h (Figures 15(e) and 16(e)), the bright material was clustered into peaks and was well delimited from the dark area. "Bee structure," as the name suggests, the asphaltene content forms highly varying light and dark interleaving bee tail structure with the increase in aging.

Based on the previous findings, it was found that the base asphalt did not appear to have a "bee-like structure" in this observation, which may be caused by the flocculation

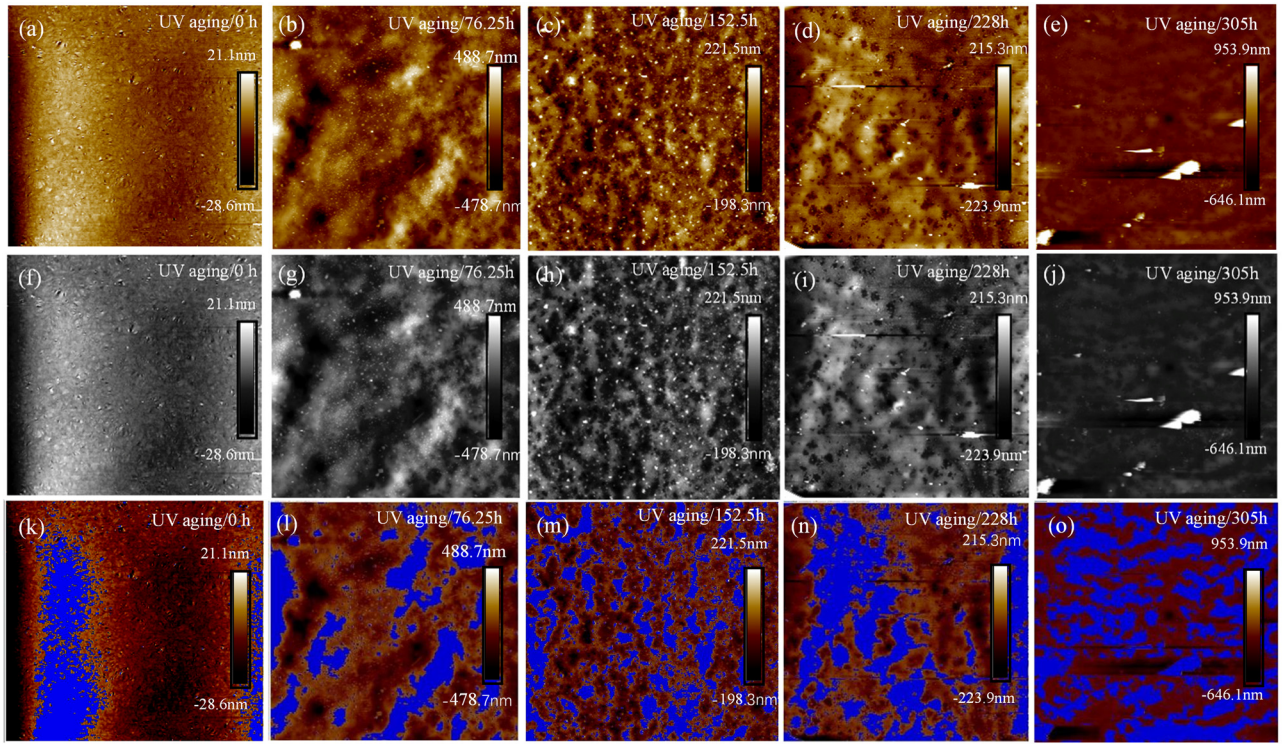


**Figure 15:** The AFM-2D characterization results and gray level images of base asphalt under different UV aging times (80 μm × 80 μm): (a) AFM-0 h, (b) AFM-76.25 h, (c) AFM-152.5 h, (d) AFM-228 h, (e) AFM-305 h, (f) Grayscale-0 h, (g) Grayscale-76.25 h, (h) Grayscale-152.5 h, (i) Grayscale-228 h, (j) Grayscale-305 h, (k) Processing chart-0 h, (l) Processing chart-76.25 h, (m) Processing chart-52.5 h, (n) Processing chart-228 h, and (o) Processing chart-305 h.

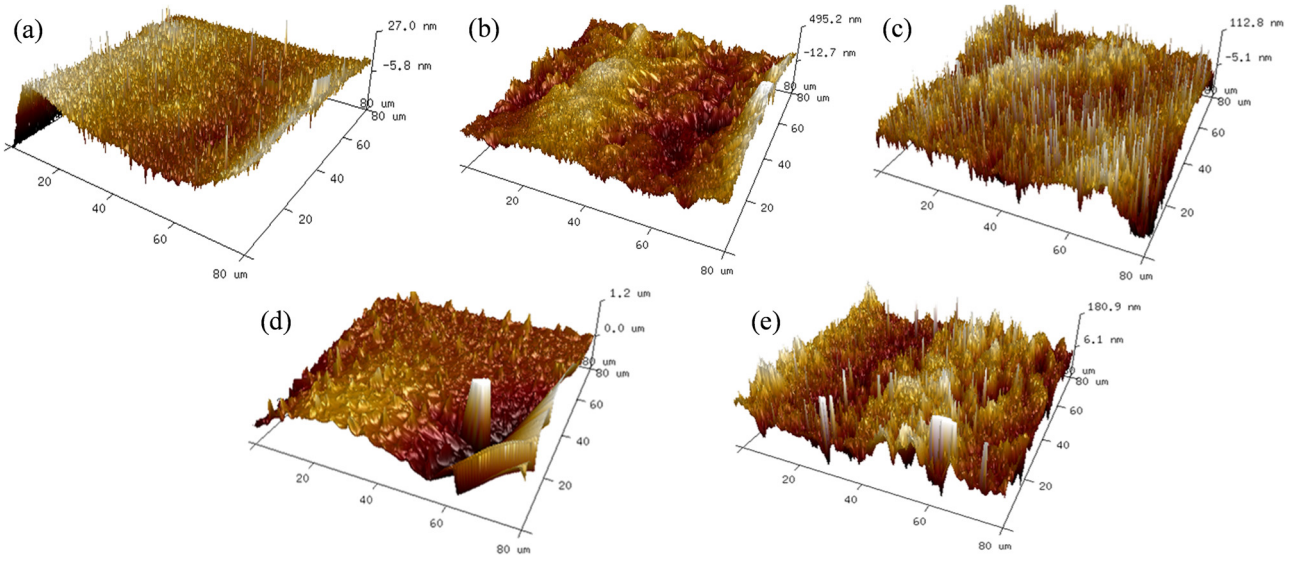


**Figure 16:** AFM-3D characterization of asphalt substrates with different UV aging times (80 μm × 80 μm): (a) 3D-0 h, (b) 3D-76.25 h, (c) 3D-152.5 h, (d) 3D-228 h, and (e) 3D-305 h.

and melting of asphaltene caused by UV aging, resulting in the disappearance of bee structure degradation [26,27]. The base asphalt was prolonged with UV aging time. With the increase in UV aging time, there were "needle structures" and "columnar structures" in the evolution of the surface morphology of the base asphalt. Subsequent studies show that "columnar structure" was also consistent with the change process of asphalt physicochemical properties during the formation of "bee structure." Relevant studies have found that the formation of asphalt's microscopic characteristic structure was influenced by the joint action of asphaltene, wax, and other components [28,29], and the change in components will accelerate the aging rate of asphalt and thus affect the change in AFM micro-structure [30,32]. It can be concluded that the morphological change in "Columnar structure" can also be used as a quantitative index to analyze the change law of asphaltene content.

The characteristic morphology was summarized by AFM characterization method to quantify the aging effect of UV radiation on asphalt binder. According to the above-mentioned characteristics of AFM, it can be seen that the area percentage of "columnar structure" (bright field part) in 2D micro-structure was selected as the quantitative index of asphalt UV aging.

As is shown in the table, the area percentage of asphalt columnar structure was 25.68% after UV aging for 76.25 h. At this point, asphalt's lightweight components have not volatilized or transformed into recombination components, and the "acicular structure" generally shows a peaceful state. With the further extension of UV aging time, the area percentage of the structure increases to 29.27%. The appearance of these data may be due to the surface depression caused by the evaporation of aromatic components in lightweight components. The other part changed from long-chain alkanes to heavy components, among which the earliest content increase was resin and part of asphaltene in the recombination component, which showed "needle structure" in the 3D figure.

When the UV aging time reaches 228 h, the asphaltenes that aggregate to form depressions and protrude due to polarity show columnar structures with different heights as shown in Figure 16(c) [31]. There were apparent depressions around the structure, which reflects that the columnar structure was formed by the accumulation of lightweight components after transformation to asphaltene. After further aging to 305 h, the aggregate area of "columnar structure" was as high as 44.33%. At this time, the area proportion of "bright field" in the image reaches the maximum.

The columnar structure has a strong correlation with the UV aging degree of asphalt. As the aging time increases, asphaltene content increases and asphaltene accumulates and aggregates to form special structures, which eventually leads to an increase in structure percentage. Based on this, the micro-structural characteristics of base asphalt can be correlated with asphalt components and asphalt aging degree.

In addition, asphaltene, as an insoluble component in asphalt, leads to a decrease in asphalt fluidity and plasticity. The internal stress of asphalt accumulates, and the stress of crack structure acts on it. Finally, the macro-

morphology of asphalt pavement cracks and the asphalt viscosity increases, and the anti-low temperature performance deteriorates [24], [32–34]. Therefore, AFM characterization method can effectively evaluate the change in asphaltene content in the aging process of asphalt and then judge the UV aging degree of asphalt binder.

#### 3.1.5.2 T770-modified asphalt

Figures 17 and 18 show the AFM-2D and 3D characterization of T770-modified asphalt under different UV aging times. The unaged T770-modified asphalt analysis shows bright and dark domains with specific limits on the asphalt surface from Figure 17(a). However, according to the observation of the corresponding three-dimensional Figure 18(a), it was found that the main reason for the area fragmentation was the uneven surface of asphalt. At this time, the bright field in the image can only indicate that there was a large area of bulge in this area. When the UV aging time was extended to 76.25 h (Figure 17(b)), many bright spots appeared at the junction of bright and dark domains. From the 3D topography (Figure 18(b)), it can be seen that the bright spots at the junction were actually "needle structures" with small diameters and dense distribution. The relatively flat asphalt surface morphology may be caused by the heat carried by UV light, which leads to the flow of asphalt components because the T770 modifier in the modified asphalt can inhibit the lightweight components in the asphalt, especially the oxidation and condensation of aromatic components, to reduce the loss of lightweight components, resulting in a low degree of asphalt aging. In short, the asphalt surface at this stage was less undulating.

When UV aging time was 228 h (Figure 17(d)), it can be seen from the image that bright fields on the asphalt surface gather and connect to form a closed and irregular shape. This phenomenon may be caused by the photo-oxidation reaction of asphalt under the coupling effect of UV light and temperature [34–37]. When UV aging time reaches 305 h, Figure 18(e) shows that many raised structures were distributed on the asphalt surface, and the "Columnar structure" increases with the dark area. At this point, the height of columnar structure of asphalt surface is relative to the average.

Similarly, to quantify the aging degree of T770-modified asphalt under UV radiation, the aging development process was evaluated by the area percentage change of "columnar structure" (bright colored area), a quantitative

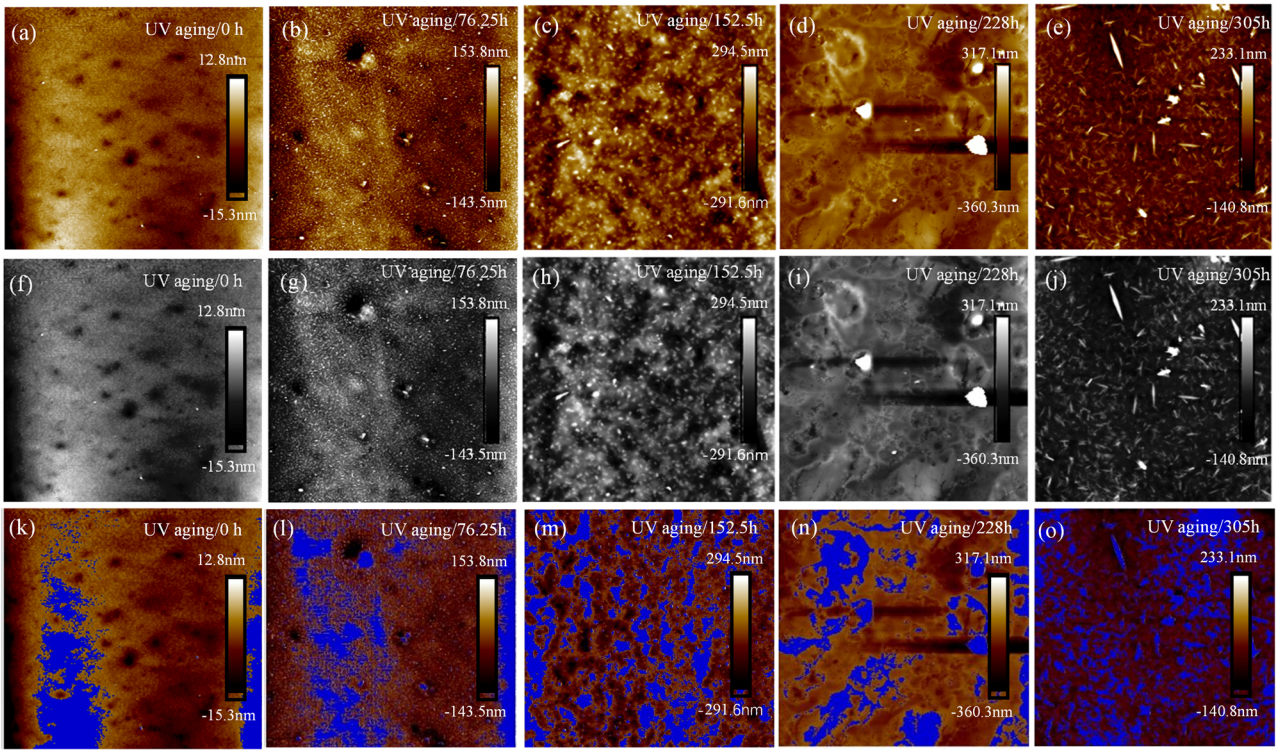


**Figure 17:** The AFM-2D characterization results and gray level images of T770 modified asphalt under different UV aging times (80 μm × 80 μm): (a) AFM-0 h, (b) AFM-76.25 h, (c) AFM-152.5 h, (d) 2AFM-228 h, (e) AFM-305 h, (f) Grayscale-0 h, (g) Grayscale-76.25 h, (h) Grayscale-152.5 h, (i) Grayscale-228 h, (j) Grayscale-305 h, (k) Processing chart-0 h, (l) Processing chart-76.25 h, (m) Processing chart-52.5 h, (n) Processing chart-228 h, and (o) Processing chart-305 h.

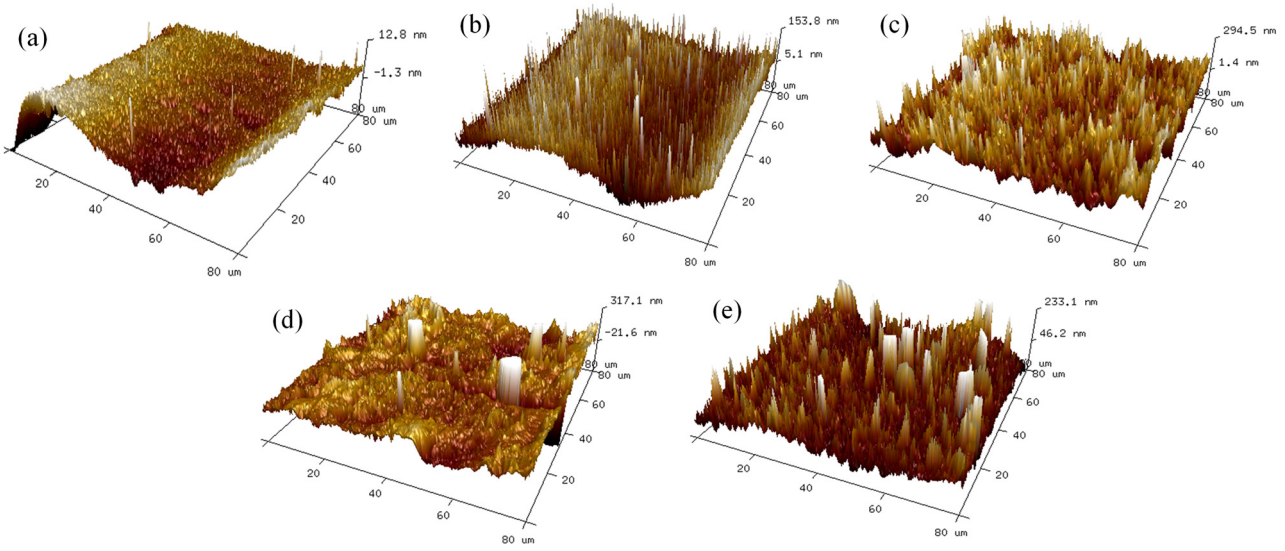


**Figure 18:** AFM-3D characterization of asphalt substrates with different UV aging times (80 μm × 80 μm): (a) 3D-0 h, (b) 3D-76.25 h, (c) 3D-152.5 h, (d) 3D-228 h, and (e) 3D-305 h.

index. As seen from the analysis of Tables 8 and 9, the area percentage of columnar structure increases significantly with the extension of UV aging time. The percentage of structure area was 22.42% at 76.25 h UV aging, which was smaller than that of base asphalt at the same time. This shows that T770 light stabilizer can maintain the stability of asphalt binder under UV radiation. When the UV aging reaches 152.5 h, the area percentage of columnar structure is 23.40%. While at the 228 h aging stage, the area percentage of columnar structure was 24.05%. When the UV aging time reaches 305 h, the percentage of structure area reaches 28.73%, and the percentage of structure area increases.

In conclusion, through the change in percentage of asphalt bright field area in each stage, the volatilization of lightweight components and the change process of heavy components in asphalt in the UV aging process can be seen. The change process of micro-structure of asphalt recombination components gradually aggregated with aging can further analyze the degree of asphalt affected by aging.

#### 3.1.5.3 T622-modified asphalt

Figures 19 and 20 show the AFM-2D and 3D characterization results of T622-modified asphalt under different UV aging times. In the observation diagram of unaged modified asphalt (Figure 19(a)), the boundaries of light and dark areas were blurred. Combined with the 3D diagram (Figure 20(a)), it can be seen that the uneven surface of whole asphalt sample caused the fluctuation changes at this stage. When the UV aging time was 76.25 h (Figure 19(b)), the boundary between bright and dark areas on the surface appeared blurred, and there was a mixed distribution of light and dark areas. In general, the dark area surrounds the bright area. The 3D diagram clearly shows this situation (Figure 19(b)). In the corresponding region, the bright region was a towering convex structure with a peak shape, while the dark region was an enveloping depression, resulting in a greater height difference. When UV aging time reaches 152.5 h, it can be seen from the analysis in Figure 19(c) that the microscopic surface development of modified asphalt was complex. According to the 3D map topography in Figure 20(c), bright particles on the surface of modified asphalt were evenly

**Table 8:** Percentage of base asphalt structure area

| UV aging time (h) | Area ($nm^2$) | Structural area percentage |
|---|---|---|
| 0 | 1310.55 | 20.02 |
| 76.25 | 1643.55 | 25.68 |
| 152.5 | 1873.44 | 29.27 |
| 228 | 2411.62 | 37.68 |
| 305 | 2837.01 | 44.33 |

**Table 9:** T770 percentage of modified asphalt structure area

| UV aging time (h) | Area ($nm^2$) | Structural area percentage |
|---|---|---|
| 0 | 1149.32 | 17.95 |
| 76.25 | 1505.47 | 22.42 |
| 152.5 | 1447.07 | 23.40 |
| 228 | 1539.16 | 24.05 |
| 305 | 1838.77 | 28.73 |

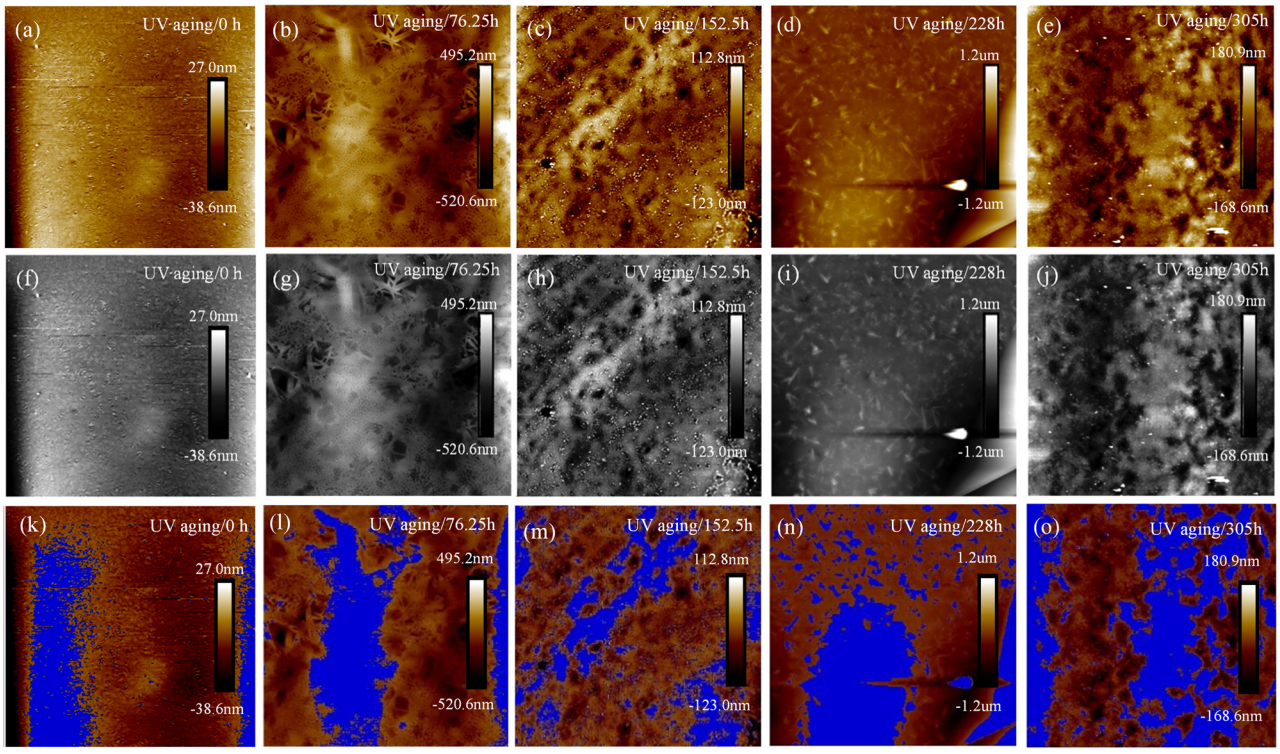


**Figure 19:** The AFM-2D characterization results and gray level images of T622 modified asphalt under different UV aging times (80 μm × 80 μm): (a) AFM-0 h, (b) AFM-76.25 h, (c) AFM-152.5 h, (d) AFM-228 h, (e) AFM-305 h, (f) Grayscale-0 h, (g) Grayscale-76.25 h, (h) Grayscale-152.5 h, (i) Grayscale-228 h, (j) Grayscale-305 h, (k) Processing chart-0 h, (l) Processing chart-76.25 h, (m) Processing chart-52.5 h, (n) Processing chart-228 h, and (o) Processing chart-305 h.

distributed and accompanied by many acicular structures. In the subsidence area representing the dark region, there were also reverse "acicular structures" with small diameters and high heights. However, due to the similar fluctuation degree of the modified asphalt, the overall height distribution was uniform and the subsidence, and uplift structure, was reduced. The structure as a whole presents a gentle surface.

When UV aging time reaches 228 h (Figure 19(d)), the asphalt micro-structure appears as a cluster of bright colored patch. In the 3D image (Figure 20(d)), it was shown

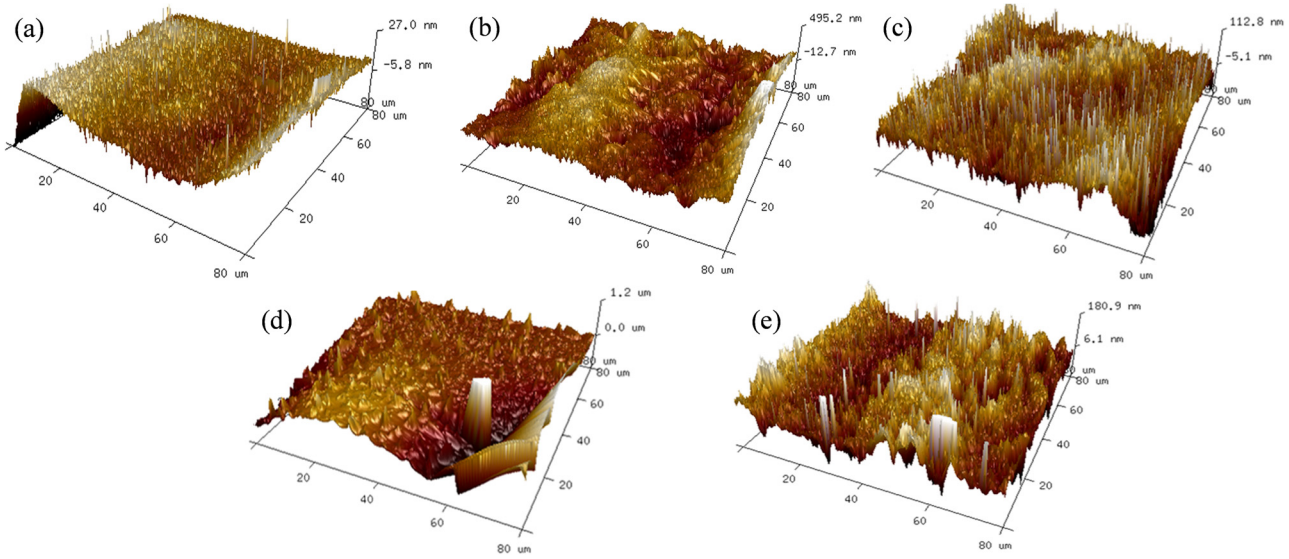


**Figure 20:** AFM-3D characterization of asphalt substrates with different UV aging times (80 μm × 80 μm): (a) 3D-0 h; (b) 3D-76.25 h; (c) 3D-152.5 h; (d) 3D-228 h; and (e) 3D-305 h.

**Table 10:** T622 percentage of modified asphalt structure area

| UV aging time (h) | Area ($nm^2$) | Structural area percentage (%) |
|---|---|---|
| 0 | 1509.86 | 23.59 |
| 76.25 | 1839.16 | 28.73 |
| 152.5 | 1803.61 | 28.18 |
| 228 | 2138.38 | 33.41 |
| 305 | 2612.6 | 40.82 |

as a "columnar structure" with a difference of 1.2 μm. When the aging time reaches 305 h, as shown in Figure 20(e), the asphalt surface shows a precise color distribution of light and dark, presenting a complex morphology of columns and valleys. Therefore, it was speculated that the source of recombination component accumulation required for columnar structure formation was provided by the light-weight components around.

The "columnar structure" in the 2D image was selected for further quantitative evaluation of the aging degree of the subsequent T622-modified asphalt, as shown in Table 10. In the whole UV aging process, the percentage of columnar structure of unaged T622-modified asphalt was 23.59%. After UV aging for 76.25 h, the area percentage of T622 modified asphalt columnar structure was 28.73%. After the aging time of 152.5 h, the proportion drops to 28.18%, which may be caused by the fact that T622 light stabilizer itself, as an additive with macromolecular structure, will cause liquidity loss in the early stage of asphalt mixing [35].

With the change in aging time, the modifier gradually decomposes and plays its role in inhibiting UV aging, reflected in the decrease in the structure percentage. The subsequent aging evaluation proved the anti-aging effect of T622 light stabilizer. When UV aging time reached 228 h, the structure percentage of T622-modified asphalt was only 88.67% of base asphalts. When UV aging time reaches 305 h, the area ratio of columnar structure was 40.82%, which was much lower than that of base asphalt (44.33%) under the same conditions. It can be seen that the photostable modifier T622 has specific anti-aging properties, and the micro-morphology change of modified asphalt was relatively complex, which was related to its complex chemical structure [35]. Therefore, the addition of a macromolecular HALS increases the viscosity of asphalt. In addition, the degradation of T622 modifier under UV light will affect the rate of asphaltene precipitation and reduce the interaction between asphalt and polymer.

### 3.1.6 Comparative analysis of the characteristics and micro-morphology of modified asphalt under the same UV aging time

The aging morphology characteristics of different types of asphalt in the non-aging stage have certain similarities, and these similarities were different in the subsequent continuous aging process. The evolution process of UV

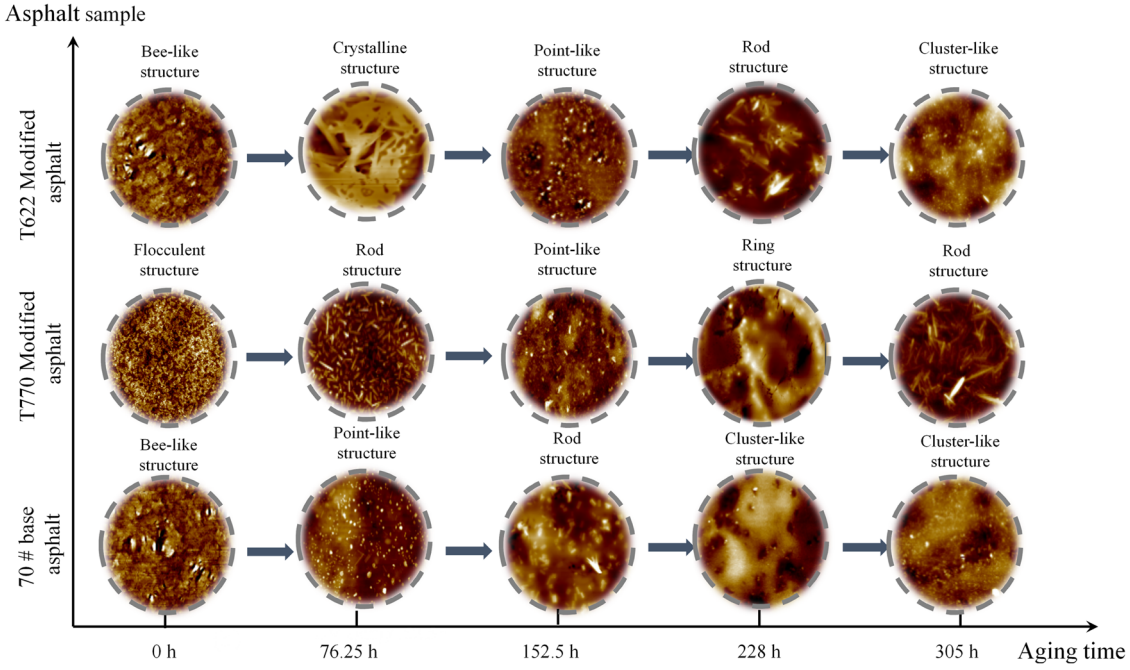


**Figure 21:** Aging evolution of three asphalt specimens (30 μm × 30 μm).

aging is shown in Figure 21. The UV aging process of base asphalt was similar to that of T622-modified asphalt, which can be summarized into four stages: "bee structure," "spot structure," "rod structure," and "group structure." The UV aging evolution process of T770-modified asphalt can be described as: "flocculent structure" – "point structure" – "rod structure" – "ring structure" – "rod structure." In the early stage of the three evolutionary processes, the "point structure" was aggregated to form the "rod structure." With the deepening of aging, the base asphalt and T622-modified asphalt first aggregate to complete the evolution of "group structure." However, the aggregate process of T770 modified asphalt was stopped, forming an incomplete "ring structure" and then back to "rod-like structure."

In conclusion, UV aging results in the AFM morphology change of asphalt, and the bright field expands gradually with aging time, and this change increases and decreases with the change in asphaltene content. The AFM characterization method found that the evolution process of base asphalt was similar to that of T622-modified asphalt. The unique evolution process of T770-modified asphalt also indicates that T770 light stabilizer has a remarkable anti-aging ability.

## 3.2 AFM roughness index analysis

The change in asphalt roughness can reflect the transformation and aging degree of asphalt components. Especially under the influence of UV radiation, the molecular structure of asphalt was damaged, and the molecular weight was reduced, resulting in the asphalt roughness being affected by macromolecular substances in the early stage and asphaltene in the later stage [38,39]. In research, the evaluation indexes usually used on asphalt roughness are Image Surface Area Difference (ISAD), arithmetic mean deviation of contour ($R_a$), and root mean square deviation of contour mean line ($R_q$). The calculation formula is shown in Table 11.

$$\mathrm{ISAD} = \frac{S_{3D} - S_{2D}}{S_{2D}}, \tag{3}$$

$$R_a = \frac{1}{l}\int_0^1 |y|\mathrm{d}x, \tag{4}$$

$$R_q = \sqrt{\frac{1}{l}\int_0^l z^2(x)\mathrm{d}x}. \tag{5}$$

The source of rough indicators is shown in Eqs. (3)–(5). Among them, ISAD is the 3D total observed area of AFM topographic map, which can be used to analyze the fluctuation of the 3D micro-structure of AFM. $S_{3D}$ and $S_{2D}$ are the total observed area of 3D and 2D AFM topography map, respectively. $R_a$ refers to the average value of the absolute distance between each point on the contour and the midline of the contour within a certain sampling length. $l$ is the sampling length. $y$ is the arithmetic mean of the absolute value of the contour margin. $R_q$ is the square root of the mean sum of the squares of all $Z$ values over a sampling length. $Z$ is the value in the $z$ direction of the roughness.

Table 11 and Figure 22 show that the asphalt roughness evaluation indexes of all three asphalt materials have peaks in specific periods. The occurrence of peak value might be related to the composition change of asphalt material under UV radiation.

Figure 21(b) shows that the $R_a$ roughness index shows the first "peak" when T622 modified asphalt and base asphalt were aged for 76.25 h. It indicates that the change in asphalt composition may cause the change. In addition, the asphalt surface morphology and structure change may be affected by the volatilization of lightweight components, and the damage to macromolecular structure was not noticeable. The subsequent reduction in roughness may be due to the relatively flat micro-structure of asphalt surface caused by the recombination fraction filling the gap caused by the loss of lightweight components [25]. In contrast, the roughness $R_a$ value of T770-modified asphalt (Figure 21(b)) does not have the same peak value. This

**Table 11:** Theoretical analysis of surface roughness before and after aging parameter statistics

| Aging time (h) | ISAD (%) | | | $R_a$ (nm) | | | $R_q$ (nm) | | |
|---|---|---|---|---|---|---|---|---|---|
| | 70# base asphalt | T770 | T622 | 70# base asphalt | T770 | T622 | 70# base asphalt | T770 | T622 |
| 0 | 0.00713 | 0.001 | 0.009 | 5.00 | 2.80 | 5.87 | 6.47 | 3.65 | 8.01 |
| 76.25 | 1.49 | 1.08 | 1.31 | 97 | 32.3 | 102 | 128 | 41.7 | 133 |
| 152.5 | 0.993 | 0.940 | 0.478 | 44.1 | 61.2 | 22.9 | 58.2 | 79.3 | 30.8 |
| 228 | 0.799 | 0.866 | 1.95 | 47.6 | 57.9 | 174 | 70.8 | 139 | 272 |
| 305 | 3.88 | 0.678 | 0.458 | 67.2 | 30.9 | 38.5 | 164 | 48 | 57.1 |

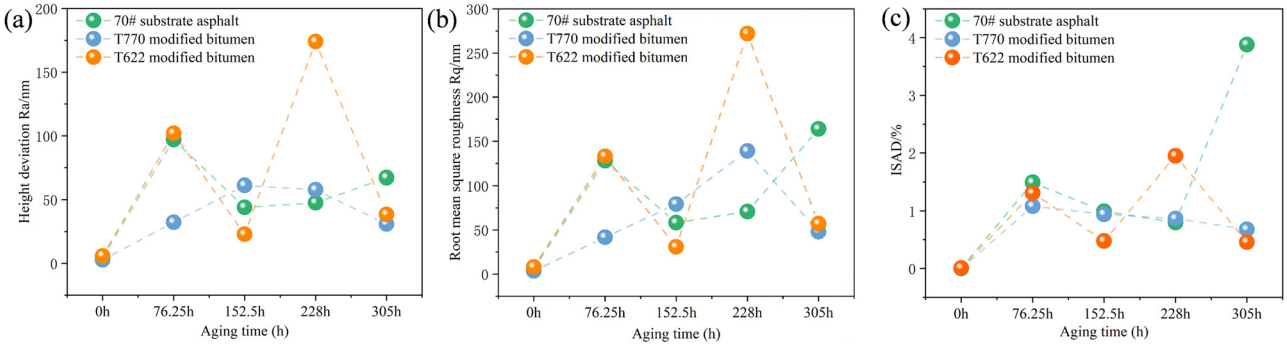


**Figure 22:** Variation in AFM roughness index: (a) ISAD diagram; (b) $R_a$ diagram; and (c) $R_q$ diagram.

effect may be caused by the small molecular structure of the T770 light stabilizer, which leads to the loss of lightweight components caused by aging being filled by small molecules of the modifier. The flow action of small molecules reduces the influence of asphalt aging, resulting in minor surface roughness deviation. This result can also be verified by the relatively low ISAD index of T770-modified asphalt (Figure 21(a)). After 228 h of aging, the roughness index of T622-modified asphalt and base asphalt (Figure 22(b)) entered the second "peak" successively. The causes of this change may be the aggregation of heavy components and the destruction of macromolecular structure.

Combined with ISAD index (Figure 22(a)), it can be seen that T622 photo-stabilized modified asphalt material was susceptible to UV aging, and its asphaltene structure was shown as the microscopic morphology of clusters, forming the "columnar structure" in the 3D image (Figure 20(d)). The base asphalt showed a similar performance, with a slight change in index $R_a$ and a significant change in index ISAD, reflecting the transformation process from lightweight components to recombination components. At the same time, the roughness index of T770-modified asphalt (Figure 22(b)) showed a slight decrease, indicating that the degree of micro-surface fluctuation of T770-modified asphalt was low and the degree of change was small, reflecting good anti-aging performance. In contrast, the roughness index of T622-modified asphalt (Figure 22(b)) has two peaks, which may be influenced by the structural characteristics of its macromolecular polymer.

In conclusion, they are combined with the variation in the roughness values of the three asphalt materials in Table 11, it was found that the evaluation indexes of their roughness after UV radiation show an overall increasing trend (Figure 22). These results indicate that the volatilization and conversion of the lightweight components of these three asphalts were hindered, which leads to more time for the conversion of the lightweight components to the recombination components and prolongation of the aging process [40]. After aging for 305 h, the roughness $R_a$ of base asphalt, T770-modified asphalt, and T622-modified asphalt increased by 13.44, 11.0, and 6.56 times compared with that before aging and were 67.2, 30.9, and 38.5 nm, respectively. These results indicate that T622 light stabilizer has a specific anti-aging performance, but T770 light stabilizer modified asphalt has better anti-UV aging ability.

### 3.2.1 Comprehensive evaluation method of asphalt UV aging based on typical microscopic morphology and surface micro-morphological characteristics

The UV aging comprehensive evaluation method based on typical microscopic morphology and characterization results means that the evaluation method adopts SEM and AFM to analyze the anti-aging ability of asphalt materials. First, the typical structure was defined and then the aging stages of different asphalt materials were divided. Finally, the aging degree of each asphalt sample and then whether the additive has an anti-aging ability were evaluated. The typical surface micro-morphologies of 70# base asphalt, T770-modified asphalt, and T622-modified asphalt were studied by this evaluation method. The results show that HALS has a better effect on inhibiting UV aging of asphalt, and the effect of T770 photostabilizer is better than that of T622.

In addition, among the comprehensive evaluation method, the most crucial step in SEM evaluation method is determining the "network structure" as the index of quantitative analysis. Because the network structure formed by the further extension and penetration of transverse and longitudinal fracture structures were unique and usually exist in the late aging period, it has the significance of evaluation. The study found that asphalt will harden with UV aging, and the microscopic surface will become rougher and fracture, resulting in a "network structure."

In contrast, AFM technology was used to analyze the effect of HALS on the micro-structure behavior of asphalt binder under UV conditions. The steps include the following: The AFM micro-topography of asphalt material was obtained. The key step is to measure the micro-structure area ratio of asphalt surface. The degree of asphalt aging was evaluated by the structural area ratio.

The results show that the change in asphalt composition causes the change in micro-structure. The accumulation of asphaltene and volatilization of lightweight components greatly affect the phase characterization of AFM structure. In addition, based on the conclusion that the bright domain is mainly composed of asphaltene and other heavy components. It can be seen that the area of asphalt bright field increases with the increase in aging time, and its structural area ratio changes according to different aging rates.

It can be seen that the indicators of various evaluation means cannot be studied at a unified level due to the difference in test means. However, in this study, SEM and AFM are selected as the techniques for detecting the surface morphology changes of asphalt materials. The obtained typical morphology and characterization results can show the evolution process of asphalt aging in different periods. Therefore, SEM and AFM can be used as evaluation techniques at the same microscopic level to analyze and study the UV aging behavior of asphalt materials.

Finally, SEM and AFM techniques can confirm the control effect of HALS on UV aging behavior of asphalt from the microscopic level. The effect of HALS on micro-morphology of asphalt binder induced by UV light was evaluated.

# 4 Conclusion

1) Compared with the base asphalt, HALS can delay the effect of UV radiation on the asphalt;
2) Cracks, particles, folds, and network structures appear in the SEM images of UV aging modified asphalt, which are all evolved from the crack structure.
3) In the aging cycle test of asphalt, the appearance time of the network structure has a relatively obvious aging stage, so it is speculated that the network structure can be used to evaluate the degree of aging.
4) The AFM evaluation index is proposed based on the evolution process of the modified asphalt micro-structure map. Based on the statistics of the asphalt recombination fraction ratio, it is speculated that the asphalt is affected by UV aging, which leads to the increase in the recombination fraction with the aging time.
5) The variation trend of the roughness index in the microscopic characterization of different asphalt cement is different, and it is speculated that the result is affected by the structural characteristics of the added modifier itself.

In this work, the evolution process of modified asphalt based on the micro-morphology was studied, and the effect of UV aging on materials was evaluated, which provided a reference for selecting the best anti-aging modifier and extending the anti-aging stage of modified asphalt. Future studies will focus on verifying the accuracy and efficiency of the morphological evaluation.

**Acknowledgments:** The authors gratefully acknowledge the sponsorship and interests listed in the *Funding information* below.

**Funding information:** This article describes research activities mainly requested and sponsored by Shanxi Transportation Holdings Group Co., Ltd. Technical Project (19-JKKJ-20), Guangdong Basic and Applied Basic Research Foundation Project (2019A1515110348), Guangdong Provincial Natural Science Foundation Project (2019A1515011397), Guangzhou HuaHui Traffic Technology Co., Ltd Technical Project under grant number 21HK0242 and Guangdong Guan Yue Highway & Bridge Co., Ltd Enterprise Mission Project under grant number GDKTP2021009700. Guangdong Science and Technology Innovation Strategy Special Fund (Project number: pdh2021a0149, pdh2022b0161). That sponsorship and interest are gratefully acknowledged.

**Author contributions:** Xiaolong Sun and Yunchu Zhu performed the measurement and were major contributors in writing the manuscript. Jie Mao and Xiao Qin measured, analyzed, and reviewed the measured data. Xiao Qin and, Huayang Yu carried out the proof reading of this article and checked the data resource. Lijuan Li and Jiao Jin performed the revision of this article and polished the English writing. All authors have accepted responsibility for the entire content of this manuscript and approved its submission.

**Conflict of interest:** The authors state no conflict of interest.

**Data availability statement:** The datasets generated during and/or analysed during the current study are available from the corresponding author on reasonable request.

# References


[1] Zhang, R., H. Wang, J. Gao, Z. You, and X. Yang. High temperature performance of SBS modified bio-asphalt. *Constr Build Mater*, Vol. 144, 2017, pp. 99–105.

[2] Wu, S. P., L. Pang, G. Liu, and J. Q. Zhu. Laboratory study on ultraviolet radiation aging of bitumen. *Journal of Materials in Civil Engineering*, Vol. 22, 2010, pp. 767–772.

[3] Yu, H. N., D. Yao, G. P. Qian, X. B. Jun Cai, X. B. Gong, and L. G. Cheng. Effect of ultraviolet aging on dynamic mechanical properties of SBS modified asphalt mortar. *Construction and Building Materials*, Vol. 281, 2021, id. 122328.

[4] Fernández-Gómez, W. D., H. R. Quintana, and F. R. Lizcano. A review of asphalt and asphalt mixture aging: Una revisión. *Ingenieria e investigacion*, Vol. 33, No. 1, 2013, pp. 5–12.

[5] Chang, J., B. Tian, L. Li, and Y. F. Zheng. Microstructure and damping property of polyurethane composites hybridized with ultraviolet absorbents. *Advances in Materials Science and Engineering*, Vol. 9624701, 2018, pp. 1687–8434.

[6] Adcock, J. L., P. S. Francis, and N. W. Barnett. Acidic potassium permanganate as a chemiluminescence reagent – a review. *Anal Chim Acta*, Vol. 601, 2017, pp. 36–67.

[7] Zhang, Y., C. Si, T. Fan, Y. Zhu, S. Li, S. Ren, and P. Lin. Research on the optimal dosage of bio-oil/lignin composite modified asphalt based on rheological and anti-aging properties. *Construction and Building Materials*, Vol. 389, 2023, id. 131796.

[8] Wang, F., Y. Xiao, P. D. Cui, J. T. Lin, M. L. Li, and Z. W. Chen. Correlation of asphalt performance indicators and aging degrees: A review. *Construction and Building Materials*, Vol. 250, 2020, id. 118824.

[9] Liu, H. B., Z. Q. Zhang, Z. N. Tian, N. Q. Li, H. W. Li, and P. F. Wang. Optimization of the evaluation indexes for asphalt ultraviolet aging behaviors based on multi-scale characterization methods: from the evolution of their physical-chemical properties and microscope morphology. *Construction and Building Materials*, Vol. 347, 2022, id. 128532.

[10] Sun, X. L., Q. Y. Peng, Y. Q. Zhu, Q. Chen, J. S. Yuan, and Y. C. Zhu. Effects of UV aging on physical properties and physicochemical properties of ASA polymer-modified asphalt. *Advances in Materials Science and Engineering*, Vol. 2022, 2022, pp. 1–12.

[11] Sun, X. L., Q. Xu, G. T. Fang, Y. Q. Zhu, Z. B. Yuan, Q. Chen, et al. Effect investigation of ultraviolet ageing on the rheological properties, micro-structure, and chemical composition of asphalt binder modified by modifying polymer. *Advances in Materials Science and Engineering*, Vol. 2022, 2022, pp. 1–19.

[12] Sun, X. L., J. S. Yuan, Y. K. Zhang, Y. M. Yin, J. B. Lv, and S. Jiang. Thermal aging behavior characteristics of asphalt binder modified by nano-stabilizer based on DSR and AFM. *Nanotechnology Reviews*, Vol. 10, 2021, pp. 1157–1182.

[13] Liu, Z. S., X. L. Sun, X. Qin, and Y. M. Yin. Micro-analysis of the fusion process between light stabilizer and asphalt using different characterizing methods. *Construction and Building Materials*, Vol. 287, 2021, id. 123045.

[14] Chen, Z. H., H. L. Zhang, and H. H. Duan. Investigation of ultraviolet radiation aging gradient in asphalt binder. *Construction and Building Materials*, Vol. 246, 2020, id. 118501.

[15] Zeng, W. B., S. P. Wu, L. Pang, H. H. Chen, J. X. Hu, Y. H. Sun, et al. Research on ultra violet (UV) aging depth of asphalts. *Construction and Building Materials*, Vol. 160, 2018, pp. 620–627.

[16] Xing, C. W., L. P. Liu, Y. Cui, and D. Ding. Analysis of base bitumen chemical composition and aging behaviors via atomic force microscopy-based infrared spectroscopy. *Fuel*, Vol. 264, 2020, id. 116845.

[17] Mokhtari, A., H. D. Lee, R. C. Williams, C. A. Guymon, J. P. Scholte, and S. Schram. A novel approach to evaluate fracture surfaces of aged and rejuvenator-restored asphalt using cryo-SEM and image analysis techniques. *Construction and Building Materials*, Vol. 133, 2017, pp. 301–313.

[18] Hung, A. M. and E. H. Fini. Surface morphology and chemical mapping of ultraviolet-aged thin films of bitumen. *ACS Sustainable Chemistry & Engineering*, Vol. 8, 2020, pp. 11764–11771.

[19] Hung, A. M., M. Kazembeyki, C. G. Hoover, and E. H. Fini. Evolution of morphological and nanomechanical properties of bitumen thin films as a result of compositional changes due to ultraviolet radiation. *ACS Sustainable Chemistry & Engineering*, Vol. 21, No. 21, 2019, pp. 18005–18014.

[20] Yu, H. N., X. P. Bai, G. P. Qian, H. Wei, X. Gong, J. Jin, et al. Impact of Ultraviolet Radiation on the Aging Properties of SBS-Modified Asphalt Binders. *Polymers*, Vol. 11, No. 7, 2019, id. 1111.

[21] Zhang, M. Y., X. C. Wang, W. G. Zhang, and L. T. Ding. Materials study on the relationship between nano-morphology parameters and properties of bitumen during the ageing process. *Materials*, Vol. 13, No. 6, 2020, id. 13061472.

[22] Zhang, H. T., Y. Wang, T. J. Yu, and Z. Q. Liu. Microstructural characteristics of differently aged asphalt samples based on atomic force microscopy (AFM). *Construction and Building Materials*, Vol. 255, 2020, id. 119388.

[23] Li, Z. Z., C. G. Fa, H. Y. Zhao, Y. Y. Zhang, H. X. Chen, and H. W. Xie. Investigation on evolution of bitumen composition and microstructure during aging. *Construction and Building Materials*, Vol. 244, 2020, id. 118322.

[24] Lyu, L., D. Li, Y. X. Chen, Y. F. Tian, and J. Z. Pei. Dynamic chemistry based self-healing of asphalt modified by diselenide-crosslinked polyurethane elastomer. *Construction and Building Materials*, Vol. 293, 2021, id. 123480.

[25] Sun, D. Q., F. Yu, L. H. Li, T. B. Lin, and X. Y. Zhu. Effect of chemical composition and structure of asphalt binders on self-healing. *Construction and Building Materials*, Vol. 133, 2017, pp. 495–501.

[26] Masson, J. F., V. Leblond, and J. Margeson. *S Bundalo-Perc Low-temperature Bitumen stiffness and viscous paraffinic nano- and micro-domains by cryogenic AFM and PDM Journal of Microscopy*, Vol. 227, 2007, pp. 191–202.

[27] Moraes, M. B., R. B. de, R. A. Pereira, L. Simão., M. Figureueiredo, Leite., et al. High temperature AFM study of CAP 30/45 pen grade Bitumen. *Journal of Microscopy*, Vol. 239, No. 1, 2010, pp. 46–53.

[28] Schmets, A. J. M., N. Kringos, T. Pauli, P. Redelius, and T. Scarpas. On the existence of wax-induced phase separation in Bitumen. *International Journal of Pavement Engineering*, Vol. 11, No. 6, 2010, pp. 555–63.

[29] Li, Y. Y., S. P. Wu, Q. T. Liu, J. Xie, H. C. Li, Y. Dai, et al. Aging effects of ultraviolet lights with same dominant wavelength and different wavelength ranges on a hydrocarbon-based polymer (asphalt). *Polymer Testing*, Vol. 75, 2019, pp. 64–75.

[30] Sun, S. S., Y. M. Wang, and A. Q. Zhang. Study on anti-ultraviolet radiation aging property of $TiO_2$ modified asphalt. *Advanced Materials Research*, Vol. 306–307, 2011, pp. 951–955.

[31] Dai, Z., J. N. Shen, P. C. Shi, H. Zhu, and X. S. Li. Nano-sized morphology of asphalt components separated from weathered asphalt binders. *Construction and Building Materials*, Vol. 182, 2018, pp. 588–596.
[32] Cao, Z. L., M. Z. Chen, J. Y. Yu, and X. B. Han. Preparation and characterization of active rejuvenated SBS modified Bitumen for the sustainable development of high-grade asphalt pavement. *Journal of Cleaner Production*, Vol. 273, 2020, id. 123012.
[33] Xiao, M. M. and L. Fan. Ultraviolet aging mechanism of asphalt molecular based on microscopic simulation. *Construction and Building Materials*, Vol. 319, 2022, id. 126157.
[34] Li, C., A. Rajib, M. Sarker, R. H. Liu, E. H. Fini, and J. M. Cai. Balancing the aromatic and ketone content of bio-oils as rejuvenators to enhance their efficacy in restoring properties of aged bitumen. *ACS Sustainable Chemistry Engineering*, Vol. 20, 2021, pp. 6912–6922.
[35] Ma, B. K., Y. J. Shi, N. Jiang, Y. M. Yang, Y. T. Yang, C. Qian, et al. A novel method for the direct detection of light stabilizer Tinuvin 622 in polymer additives by gel permeation chromatography combined with multi-angle laser light scattering. *Talanta*, Vol. 253, 2023, id. 123896.
[36] Falchetto, A. C., A. Montepara, G. Tebaldi, and M. O. Marasteanu. Microstructural characterization of asphalt mixtures containing recycled asphalt material. *Journal of Materials in Civil Engineering*, Vol. 25, 2013, pp. 45–53.
[37] Qian, G. P., G. C. Yuan, D. M. Zhang, and Z. J. Li. Effect of composite light stabilizer on the anti- ultraviolet aging property of base asphalt. *Journal of Materials in Civil Engineering*, Vol. 33, No. 8, 2021, p. 04021176.
[38] Zhang, H. L., J. Y. Yu, Z. G. Feng, L. H. Xue, and S. P. Wu. Effect of aging on the morphology of bitumen by atomic force microscopy. *Journal of Microscopy*, Vol. 246, No. 1, 2012, pp. 11–19.
[39] Tang, Z. P., F. L. Huang, and H. Peng. Effect of 3D roughness characteristics on bonding behaviors between concrete substrate and asphalt overlay. *Construction and Building Materials*, Vol. 270, 2021, id. 121386.
[40] Ma, F., Y. J. Wang, Z. Fu, Y. J. Tang, J. S. Dai, C. Li, et al. Thermal ageing mechanism of a natural rock-modified asphalt binder using Fourier transform infrared spectroscopy analysis. *Construction and Building Materials*, Vol. 335, 2022, id. 127.